Chapter 14
Advanced Bonding Technology Based on Nano- and Micro-metal Pastes

Katsuaki Suganuma and Jinting Jiu

Abstract With the development of silicon carbide (SiC) high-power semiconductor devices, which have the advantages of lower power losses, higher efficiencies, higher thermal conductivities, and higher operational temperatures compared to traditional silicon-based power devices, the demand for high-temperature bonding materials is becoming extremely urgent. The transition liquid phase (TLP) method has been used to form intermetallic compounds (IMCs) to bond SiC devices, and the IMCs formed by the TLP method have been studied as replacements for traditional low-temperature solder materials. However, the long process times and the high process temperatures required by the TLP method significantly damage power integrated circuits (ICs), and unstable IMCs cause reliability problems in the service process. Recently, metal particle pastes have been developed for high-power devices application, and these pastes have proven to be a feasible means of achieving high performance.

A review of recent advances in the development of metal pastes for bonding technology is provided in this chapter. The basic bonding technology, fundamental concepts of metal pastes, and the fabrication processes of pastes are introduced. The effect of nano- and micro-Ag pastes on the performance and reliability of the obtained joints is addressed in detail. The development of copper (Cu) pastes and its various anti-oxidation strategies are also summarized. Some precautions and propositions improving the strength and reliability of joints are also presented. Finally, at the end of the chapter, the direct-bonding method based on metal films is also discussed. These contents can be mainly interesting for researchers working on high-power semiconductor devices.

K. Suganuma, Ph.D. • J. Jiu, Ph.D. (✉)
The Institute of Scientific and Industrial Research (ISIR), Osaka University,
Mihogaoka 8-1, Ibaraki, Osaka 567-0047, Japan
e-mail: suganuma@sanken.osaka-u.ac.jp; jiu@eco.sanken.osaka-u.ac.jp

© Springer International Publishing Switzerland 2017

D. Lu, C.P. Wong (eds.), *Materials for Advanced Packaging*,
DOI 10.1007/978-3-319-45098-8_14

14.1 Introduction

Since the first commercialization of SiC Schottky diodes in 2001 [1], wide-bandgap (WBG) high-power semiconductor devices based on silicon carbide (SiC) and gallium nitride (GaN) have attracted much attention because of their lower power losses, higher efficiencies, higher thermal conductivities, much higher operational temperatures, higher current densities, and higher blocking voltages compared to silicon-based power devices [2–8]. Some commercially available power devices, such as junction field-effect transistors (JFETs), metal–oxide–semiconductor field-effect transistors (MOSFETs), and bipolar junction transistors (BJTs), are now beginning to enter the power electronics marketplace and are being applied in high-end devices, such as server and telecom power supplies, solar power conversion, hybrid vehicles, and space and military monitoring systems. The global market for WBG high-power semiconductor devices is expected to be over $3 billion in 2020.

Even though several SiC-based power devices have been successfully commercialized, the SiC device market is still in an early stage. There are still many issues that must be resolved. These include how to reduce the prices of SiC devices (which are still higher than Si devices); how to design the gate drive circuit, taking into account the unique operating characteristics of SiC in MOSFETs; and how to join the SiC dies to the chip carrier or lead frame while operating within acceptable joining temperature ranges. First among these issues, and necessary to fulfill the potential of WBG devices, interconnection technology and reliable packaging must be developed to meet the demands of high-temperature operating environments. The device based on SiC chips can be operated well over 400 °C (this is far higher than the maximum allowable junction temperature of standard silicon technology of about 150 °C), which largely decreases the cost of the cooling system, since lower cost cooling materials and methods can be used. Die-attachment materials, which physically connect the SiC chips to the rest of the system, and also provide electrical and thermal pathways for semiconductor devices, must have high electrical conductivity and must be able to operate at the high temperatures.

Traditional die-attachment materials include Sn-based solders, Pb-free solders, and conductive adhesives, and these are used widely in silicon technologies because of their desirable joining process and temperatures. However, higher-temperature applications such as hybrid electric vehicles, aircraft, and space exploration craft cannot exploit these traditional low-temperature packaging materials because they melt at around 210–250 °C [9–11]. Thus, new high-temperature, die-attachment materials must be developed in order to join SiC and/or GaN chips to various high-power, electromechanical devices.

In order to improve the service and/or operating temperatures of the die-attachment materials, a higher-melting point solder is needed. High-Pb solders are widely used as die-attachment materials due to their optimal melting temperature range (300–314 °C), low cost, excellent wettability, and workability [12, 13]. However, these materials need to be completely eliminated from

electronic applications in the near future under the restriction of hazardous substances (RoHS) directive, which was enacted to reduce lead pollution and to protect both human health and the environment. Other binary and ternary alloys, such as Au–Sn eutectic alloys [14–17], Bi–Ag alloys [18, 19], and Zn-based alloys [20–25], have been proposed as possible alternatives. Au–Sn eutectic alloys have an appropriate melting temperature of 280 °C and have excellent conductivity; however, they produce brittle intermetallic compounds (IMCs), leading to poor high-temperature reliability [17]. Besides, gold is very expensive for industrial applications. Bi–Ag alloys are very brittle in nature and show poor electrical and thermal conductivities [18, 19]. Zn–Al alloys, which have the most suitable melting range, are also brittle in nature [20, 21] and show poor thermal cycle reliability [22]. Although Zn–Sn alloys show great potential due to their superb heat cycle resistance in the range of about −40–125 °C and their high thermal conductivity, the use of Zn–Sn alloys is limited to power devices operating above 200 °C, since Zn–Sn solders undergo a partial eutectic melting reaction at about 200 °C [26]. Another serious drawback arises from the high melting points of these alloys. The high melting points lead to high joining temperatures, which damage components and cause excessive consumption of the substrates. Therefore, developing new materials, which can be joined at low temperatures, but still operated at high temperatures, has become an urgent issue for high-power devices.

There are two strategies that have been adopted to address this issue [27]. One is TLP bonding technology, which combines the characteristics of liquid phase joining (soldering and brazing) and diffusion bonding [28–33]. During this bonding process, a metal interlayer with a low melting point is diffused into a component with a high melting point in order to form IMC layers with the requisite properties for high-performance joints. The process is achieved by the use of metals with a low melting point, such as Bi–In–Sn alloys, as interlayer. An acceptable formulation may achieve bonding at low temperature; however, it is usually necessary to apply compressive stress in the beginning of the process, so as to minimize the joint gap and, furthermore, to apply a long-time heat treatment, so as to grow a homogenous joining layer. In addition, most of the IMCs are unstable and brittle; in some IMCs, Kirkendall voids at the joint reduce reliability. These factors have severely hindered the wide acceptance of TLP bonding as an alternative to high-temperature soldering.

Another promising bonding technology is based on the sintering of metal particle pastes, including those containing Ag or Cu or mixtures of these two metals [34–38]. The high melting points, high tensile strengths, low elastic moduli, and high electrical and thermal conductivities of the sintered metal particle pastes provide numerous advantages over traditional solders and alloys. Thus, many attempts have been made to use sintered metal particle pastes in the fabrication of microelectronic packages. These metal pastes can be sintered to form a continuous, bulk-like network at temperatures significantly below the melting point of bulk metal, greatly reducing manufacturing costs and simplifying bonding conditions. Furthermore, the absence of a solid–fluid phase transition in the sintering process prevents the movement and misalignment of chips and allows the exact positioning

of chips at the desired locations for optimum operational performance. This chapter will focus on the development of the sintering technology of these metal particle pastes, including silver and copper pastes. The synthetic methods of the metal pastes, the effect of bonding processes on the performance, and the reliability of joints will be addressed in detail. Some recent advances in direct joining methods based on Ag or Cu films will be mentioned in the end of the chapter.

14.2 Silver Pastes

The history of the sintering of metal particle pastes dates back to studies in the late 1980s led by Schwarzbauer and his team [39, 40]. In order to secure electronic components to a substrate, a paste, primarily composed of micron-sized Ag particles and a solvent, was printed on the substrate to make a thin layer and then dried (silver was chosen because of its high stability and high electrical conductivity compared to other metals). After components were placed on the top of the paste layer, the entire arrangement was heated to a suitable temperature, with a mechanical pressure, producing a dense and highly conductive sintered Ag joint. Other teams optimized the process of sintering micron-sized Ag particles, for example, changing the preheating stage and the heating rate, and adding silver compounds, e.g., AgO. These optimizations achieved sintering temperatures in the range of 200–350 °C and sintering pressures from several to tens MPa [41–43]. Compared to high-temperature solder, the micro-Ag joint was achieved at relatively low temperatures; hence, the process is often referred to as the "low-temperature joining technique." Although this sintering method is especially useful in component-level mounting of power semiconductors and is being used for industrial production [44], a quasi-hydrostatic pressure of 30–50 MPa requires specialized tool to avoid breaking the semiconductor dies during the die-bonding process. Moreover, the temperature (generally above 250 °C) is high enough to introduce large strains and plastic deformations to the dies, leading to structural damage, especially of fine and small components. Coupled with the rapid development and many breakthroughs in various high- and low-temperature, Pb-free solders and alloys [27, 45–49], the low-temperature, Ag-based joining technique with high applied pressures no longer receives the attention as it first did in the 10 years after its invention in 1989.

14.2.1 From Micro-Ag Paste to Nano-Ag Pastes

To avoid or reduce the need for high pressure during the joining process, it is possible to use smaller-sized Ag particles. It has long been known that small particles have a natural propensity to sinter or to Ostwald ripen, as a means of reducing total free energy. This is called the Gibbs–Thomson effect. When the particle size becomes small, the number of atoms included in the particle decreases

but the ratio of surface area to volume increases. Thus, the melting points of nanoparticulate materials decrease almost linearly with the inverse of the average particle radius due to effects of the surface energy; consequently, these nanoparticle pastes are more prone to sinter at relatively low temperature [50–52]. Although numerous studies on the relationship between melting point and particle size have been performed since the first detailed experiments, which used an evaporation method to make thin metal films with thicknesses less than 100 nm, were published by Takagi in 1954, most reports only focused on theoretical simulations and calculations [52–55]. This is due to the difficulty of preparing nanoparticles with precise morphologies at large scale.

Scientific development and personal growth are similar in that opportunity drives success. Since entering the twenty-first century, nanomaterials such as nanoparticles, nanofilms, nanoflowers, nanodots, nanowires, and nanotubes have been the focus of intensive research because their unique electronic, optical, magnetic, thermal, catalytic, and other properties are distinctly different from their bulk counterparts. Much effort has been made to control their structure and morphology in order to produce materials with desirable properties [56–65]. Many methods have been developed to synthesize various metals, metal compounds, alloys, and polymer nanoparticles with narrow distributions in diameter, with special morphologies, and with high yields at large scale [66–69]. Once materials are readily available, applications for the materials become a matter of course.

14.2.2 Performance of Joints Based on Nano-Ag Pastes

The performance of power electronics depends on the structure of Ag joint formed during the sintering process of nano-Ag paste. The thermal and electrical conductivities, elastic moduli, ratcheting, and creep behaviors of the sintered nano-Ag pastes have been studied at various temperatures and stresses [70–73]. The electrical resistivity of the nano-Ag joint is lower than that of conventional solders, and values between 2.5 and 10 μΩ.cm have been reported (the electrical resistivity of bulk silver is 1.6 μΩ.cm [74–78]). Typical thermal conductivity values of sintered joints are far higher than with conventional solders and range from 200 to 300 $Wm^{-1}K^{-1}$ [79–81]. The elastic modulus based on the sintered nano-Ag is about 6–9 GPa, which is much lower than bulk silver and also lower than typical Pb–Sn or Pb-free solders because of the porous structure [82–87]. However, it is neither practical nor the aim of this research to produce a dense nano-Ag joint; rather, it is necessary to balance the elastic modulus and other mechanical properties, such as strength and fatigue properties [84, 88]. Moreover, a low modulus can also relax thermal stress and enhance durability of the electrical devices [83, 89–91]. In addition to these thermal, electrical, and mechanical properties, joint strength is another important parameter to consider when evaluating various options for sintered nano-Ag joints for high-temperature applications. The die-shear strength of a sintered nano-Ag joint was reported to be in the range of 20–70 MPa, depending on the sintered nano-Ag density and grain size.

These properties, in turn, were affected by various parameters during the bonding process, including the bonding temperature, time, and pressure, the sintering dwell time, the heating rate, the sintering atmosphere, and the properties of nano-Ag pastes, such as organic content, and the size and shape of the nanomaterials. In the following sections, we will discuss these sintering parameters and their effects on the joint strength.

14.2.2.1 Sintering Pressure in Nano-Ag Pastes

Figure 14.1 shows a schematic of a nano-Ag paste used to bond two components together. Nano-Ag pastes contain silver nanoparticles and organics. During the bonding process, these organics evaporate or decompose, releasing gas; then, neck growth occurs between adjacent particles, resulting in a porous sintered Ag structure. The release of gas during the sintering process causes voids between components and paste, and this is mitigated by applying suitable pressure. Similar to micro-Ag pastes, pressure always improves the strength of the resulting joint; thus, it is not surprising that increasing the bonding pressure for nano-Ag pastes results in bonds with higher shear strength. For example, Ide et al. reported a shear strength of 25 and 40 MPa at 300 °C, for a nano-Ag paste with average particle diameter of about 11 nm, and applied pressure of 1 and 5 MPa, respectively [92]. Morita et al. also achieved a rapid increase in shear strength with a similar nano-Ag paste, from 10 to 30 MPa, with a sintering temperature of 250 °C, when the applied pressure was changed from 0.5 to 5 MPa [93]. When the size of Ag particles was decreased to 5 nm, the shear strength was only 2 MPa with applied pressure of 5 MPa and a sintering temperature of 250 °C; raising the sintering temperature to 400 °C only increased the shear strength to 15 MPa. It indicates that the size effect is crucial except the sintering pressure and temperature. Yan et al. achieved a strength of about 20 MPa at a sintering temperature of 250 °C by using high concentration of nano-Ag paste with the particle diameters of about 40 nm; this high strength was achieved without applying any pressure. The strength was improved to about 50 MPa when 5 MPa pressure was applied [94]. These results suggest that shear strength increases significantly when the

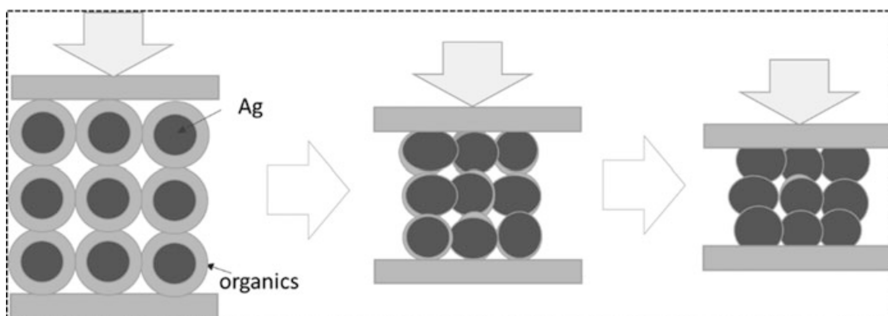

Fig. 14.1 The schematic diagram of sintering process for nano-Ag paste under pressure

bonding pressure is used even only 5 MPa. This increase can be attributed to the following: (1) better contact between the paste and the bonded substrates, (2) the rearrangement of the nano-Ag particles to form a higher packing structure, and (3) a continuous densification process due to the decomposition and removal of organics when sintering pressure is applied. However, further increases in bonding pressure to 10 MPa provided limited improvements in the strength. This seems to indicate that a threshold bonding pressure of 5 MPa exists [95]. It should be noted that this threshold pressure is also dependent on particle size; however, the direct correlation between particle size and threshold pressure remains unclear. In summary, the joint strength depends on the sintering pressure, which was effected by the size and morphology of the Ag particles in the paste.

14.2.2.2 Sintering Temperature and Time in Nano-Ag Pastes

As mentioned above, the shear strength depends on the sintering temperature [93]. This is because the sintering of the nano-Ag paste is determined by the evaporation and decomposition of the organic matter in paste, which, in turn, depends on temperature and time. After the release of organics, sintering can proceed quickly, due to the huge driving force provided by surface energy of the net particles and the applied external pressure. It has been shown that an increase of the sintering temperature and dwell time generally leads to an improvement in the shear strength along with an increase in density of the Ag structure within the joint [76, 94, 96–99]. It is easy to understand this, given that the mechanisms of evaporation and decomposition of organics in silver paste involve physical desorption processes and chemical reaction processes, and all of these processes increase with temperature. High temperatures lead to rapid evaporation, desorption, and chemical decomposition, and these processes contribute to the formation of a net surface of particles which drives the sintering process to completion. The holding time also affects joint strength [76, 96, 100]. The densification of particles, which occurs via the rapid growth of grains and pores, requires time to reach completion, as do the processes of evaporation and decomposition of organics. Above an optimal sintering temperature, further densification may have no effect or may even slightly degrade the sintered joint performance due to coarsening [76, 98, 99]. Similarly, the shrinkage of sintered Ag nanoparticles diminished after a period of time, and extending the sintering time was not worthwhile once the densification rate dropped below a certain point [76]. In fact, the influence of sintering time and temperature should be considered simultaneously. At high sintering temperatures, densifying mechanisms such as grain boundary and lattice diffusion operate to densify the nano-Ag joint [101]. If the sintering temperature is too low, a long sintering time will only result in grain growth instead of densification, and this naturally leads to lower shear strength. Moreover, the optimum sintering temperature and time are related to properties of the nano-Ag pastes, such as diameter, morphology, dispersant, and solvent, as well as to the specifics of joint design [102].

14.2.2.3 Heating Rate in Nano-Ag Pastes

Another important sintering parameter is the heating rate. It has been reported that surface diffusion is the dominant mechanism for low-temperature sintering, while grain boundary or lattice diffusion dominates the high-temperature sintering of nanopowders [103]. Although a high heating rate might minimize the aggregation of nanoparticles during the ramp-up to the high sintering temperature [95], the heating rate must be low enough to allow adequate outgassing of organics, without disrupting the connection between the nano-Ag particles. Hence, an initial pre-sintering process is always introduced to dry the paste before the actual sintering [95]. Some researchers also introduce a separate drying profile or a double printing process with an interim step of drying before the final sintering step, to ensure complete outgassing of the solvents before densification. However, a low heating rate can induce the overgrowth and aggregation of nano-Ag particles, and these larger particles then require higher sintering temperatures for densification [104]. Hence, it is necessary not only to avoid the overgrowth of particles with a high heating rate but also to release all organics with a low heating rate in the initial stages of the sintering process. Furthermore, it has been shown that a rapid heating rate results in the formation of a denser joint with higher shear strength. An excellent example of the effect of heating rate on the microstructure of sintered Ag particles is shown in Fig. 14.2 [76]. This figure shows that a low rate was

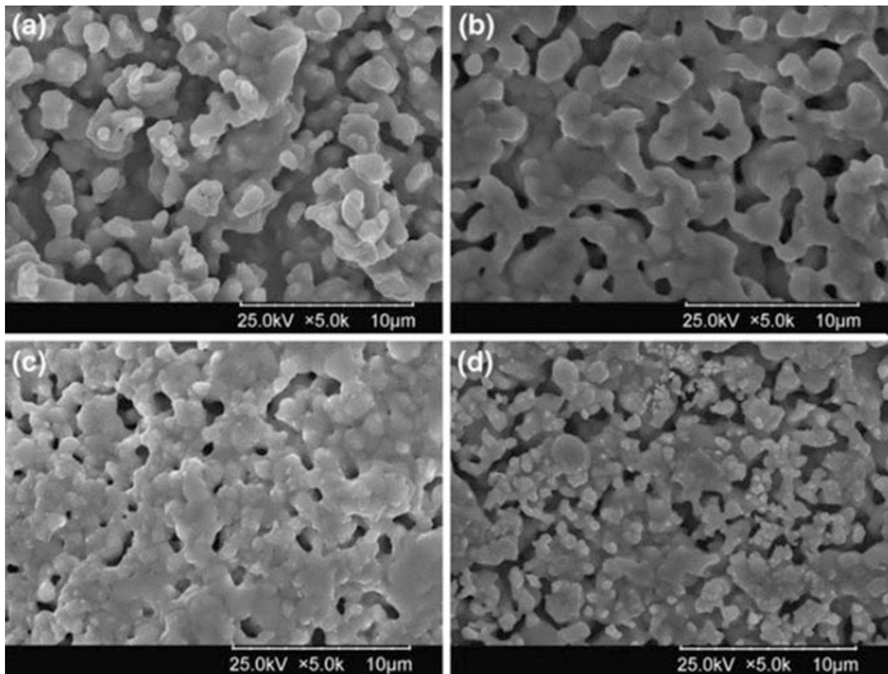

Fig. 14.2 SEM images of the fracture surface of nano-Ag joints with different heating rates: (**a**) 1, (**b**) 10, (**c**) 20 °C/min, and (**d**) direct heating [76]

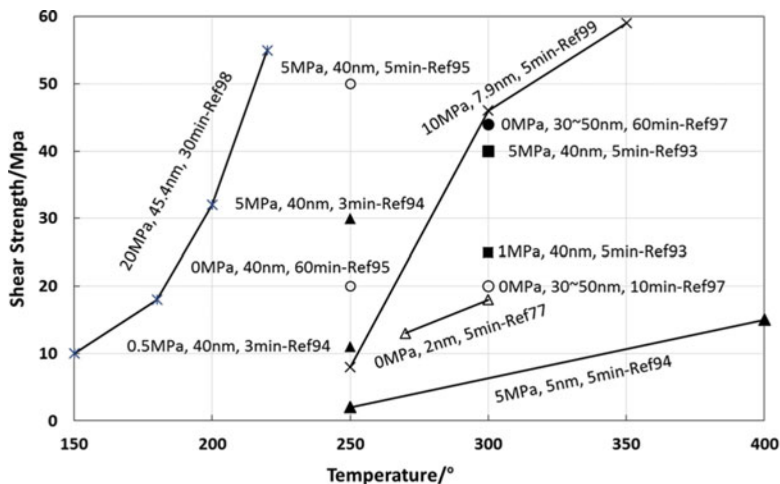

Fig. 14.3 The shear strength of nano-Ag pastes with various bonding conditions [76, 92–94, 96, 98]

beneficial for the optimum vaporization of organics in the paste; however, if Ag nanoparticles stayed too long in the low-temperature regime, the sintering driving force was consumed by non-densification processes, and this led to sintered materials of high porosity and low shear strength. When the heating rate was increased, the sintered Ag nanoparticles tended to be more compact, and, at the same time, the effective connecting area between the grains increased, contributing to high shear strength. Too high heating rate caused partial sintering and left many dried nanoparticles with their original morphologies. Therefore, in sintering process, a variable heating rate might be better able to match the surface and lattice diffusion of nano-Ag pastes.

A summary diagram is shown in Fig. 14.3, which clearly indicates how sintering parameters affect the strength of joints. The strength increases with the sintering temperature and pressure when same Ag pastes were used. Even with Ag pastes of the same composition, the strength depended on the heating rate and sintering time. On the other hand, in addition to the sintering parameters mentioned above, other factors, such as the sintering atmosphere, bonding substrates, bonding area, and composition of paste, also affect the joint strength. Detailed discussions on these aspects of nano-Ag joints can be found in recent reviews [34–36, 38].

14.2.3 From Nano-Ag Pastes to Hybrid Silver Pastes

In most die-bonding processes, applied pressures of about 1-20 MPa, even pressures over 50 MPa, are always needed to improve the bonding performance, and to increase the bonding strength of micro- and nano-Ag pastes. The development of

the latter has decreased the pressure required to about 2–5 MPa, depending to the size and type of nanoparticles in the silver pastes. Bonding joints with strengths of about 20 MPa have been achieved with no applied pressure at the high sintering temperature of 300 °C; however, the strength was decreased substantially, to only 10 MPa, far below the requirements of industrial applications, when the sintering temperature was reduced to 200 °C [94]. This is indicative of the difficulty associated with simultaneous optimization of the sintering temperature and pressure, with pastes containing nanoparticles comprised solely of silver. The primary reason for this is that nano-Ag pastes require high levels organics for dispersion and storage. Thus, there is a strong desire to reduce or eliminate the pressure required for the low-temperature sintering process for the very thin SiC/GaN chips, which might suffer from passivation cracking during pressure sintering.

In these nano-Ag pastes, the presence of organics correlates with the need for applied pressure, as shown in Fig. 14.1. In order to increase the contact area and the probability for contact between neighboring Ag particles when organics are removed, applied pressure is used to assistant and enhance the shrinkage of the Ag structure. One approach to minimize the applied pressure is to increase the concentration of Ag particles by decreasing the level of organics in the pastes. A nano-Ag paste containing 96.1 mass% Ag particles achieved high-strength Ag joints during pressureless sintering [94]. The organic content of the paste, about 3.9 mass%, was significantly lower than the 15 mass% found in conventional nano-Ag pastes [92]. However, to achieve pressureless sintering, the sintering temperature was increased to over 300 °C as a result of the grain boundary diffusion in the presence of so many silver nanoparticles. Considering the effects of pressure and temperature, just described, on the performance of silver joints, it is reasonable to expect that hybrid Ag pastes, composed of nano- and micro-sized Ag particles, might allow for an increase in the concentration of Ag particles, with a simultaneous decrease in the level of organics in the pastes. Indeed, this was observed for hybrid Ag pastes; these hybrid pastes showed a decrease in both the sintering temperature and pressure required to achieve high performance of the Ag joints [105, 106].

The sintering process of the hybrid Ag pastes is shown schematically in Fig. 14.4. When Ag particles with different diameters are mixed together, the contact opportunity and area between neighboring particles is naturally increased

Fig. 14.4 The schematic diagram of sintering process for hybrid Ag paste

due to enhanced close packing structure which is similar to the application of pressure. When the organics in the paste are removed, neck growth between adjacent particles occurs naturally, making a dense, sintered Ag structure. The neck growth occurs easily between adjacent small and large particles [107]. The advantages of a hybrid Ag paste can be summarized as follows: First, the sintering pressure decreases. Generally, pressure is required to increase the contact area between Ag particles. In the hybrid paste, Ag particles of different sizes naturally form a denser structure, and this increases the contact area. Second, the sintering temperature decreases. As particle diameters decrease into the nano-size regime, melting points decrease, allowing for easy sintering [50–52]. The presence of Ag nanoparticles in the hybrid pastes enhances sintering because grain boundary diffusion occurs readily between small and large particles [107]. Third, the level of organics in the paste is reduced. An organic coating always exists on the nanoparticle surfaces, and this prevents Ag nanoparticles from self-cohesion and agglomeration during preparation, dispersion and storage. In the hybrid paste, the addition of Ag microparticles to Ag nanoparticles decreases the concentration of Ag nanoparticles, thereby reducing the level of organics, which, in turn, promotes sintering. Fourth, costs decrease. The excessive miniaturization of nanoparticles decreases the sintering temperature; however, it significantly increases the cost of the Ag paste as well as the relative level of organics in the paste. For a hybrid Ag paste with an optimized Ag particle size distribution, one can use micrometer or sub-micrometer Ag particles to substitute those nano-Ag particles [105, 106, 108].

14.2.3.1 The Fabrication Methods of Hybrid Ag Pastes

The composition of a hybrid silver paste is simple; it consists of two or more Ag particle types, dispersed in a solvent, in order to ensure a close-packed Ag structure after sintering treatment. There are two main fabrication methods. The first is to directly mix Ag particles of different diameters. The second is to mix Ag powder and Ag compounds which decomposed into Ag nanoparticles during the sintering process. In the first method with the direct mixture of Ag microparticles and submicron Ag particles, many promising results have been reported [105, 106, 108–111]. The Ag microparticles had an average diameter of about 8 μm, and the submicron Ag particles had an average diameter of about 300 nm. The Ag microparticles had a flake-like shape and enhanced contact area between particles and substrates because of their relatively flat surfaces. The submicron Ag particles had a spherical shape with small size and could fill the voids between the Ag microparticles to make a dense Ag structure [106]. The mixing method was easy and simple to control by varying the levels of different-sized submicron Ag particles. However, the optimal matching of variously sized Ag particles with different surface coating agents, the optimization of the diameters of the various Ag particles, and an understanding of the relationships between Ag particle diameters and joint performance are issues that remain to be addressed.

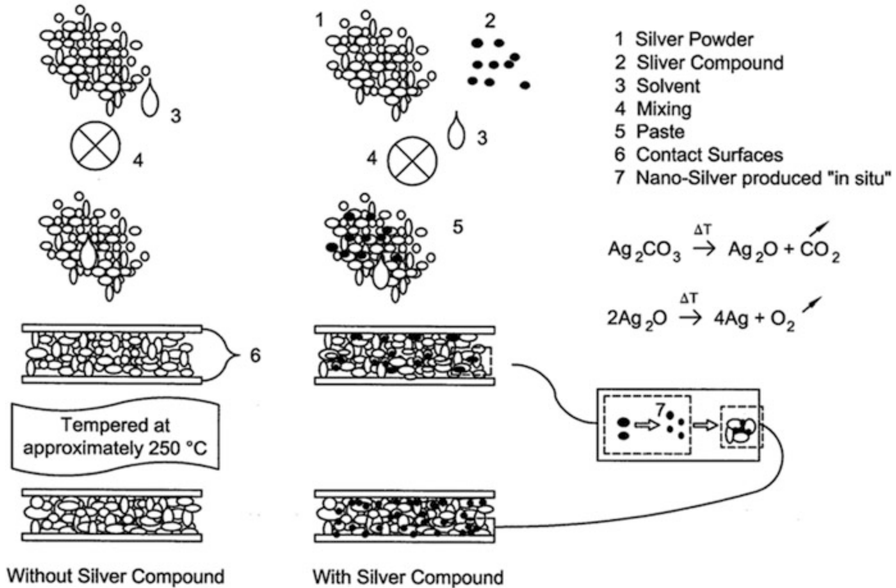

Fig. 14.5 The schematic diagram of hybrid Ag paste based on silver power and Ag compounds [112]

The second method described above, the in situ growth of small Ag particles during the sintering process, is also being evaluated as a method for producing a hybrid paste. It is known that silver oxides are thermal unstable and easily reduced to metallic Ag at temperatures above 250 °C [86]. Making use of the property of endothermic decomposition of Ag_2O, Schmitt et al. used Ag microparticles and Ag compounds to make a hybrid Ag paste [112, 113]. When the paste was heated, Ag nanoparticles were produced in situ and filled the voids between submicron Ag particles, resulting in low-temperature sintering under low pressure (Fig. 14.5). Using the in situ formation of Ag nanoparticles during the heat-driven decomposition of Ag_2O, Morita et al. directly used submicron Ag_2O particles to bond copper disks by heating at 300 °C in air under a pressure of 2.5 MPa, achieving a shear strength of about 20 MPa [114]. Problems arise due to the violent decomposition of Ag compounds during the sintering process; therefore, extra pressure is always needed to keep the chip fixed and to maintain the arrangement of various components in the device. Therefore, the first method for the direct mixture of Ag microparticles and submicron Ag particles is a promising way only if some compounds which easily decompose at low temperature are developed.

14.2.3.2 The Joint Performance and Reliability of Hybrid Ag Pastes

The performance of Ag joints depends on many factors, including the type of Ag particle, the composition of the paste, and the sintering parameters mentioned above. As for Ag nanoparticle pastes, the shear strength of joints formed by hybrid Ag pastes is generally improved by the varying properties of the hybrid Ag paste. One of the present authors has demonstrated that micron-sized Ag particles can provide a stable bonding strength at 200 °C without applying pressure [106]; when Ag particles with an average particle diameter of 300 nm were added to the hybrid Ag paste, the joint strength was greatly improved, even at low or zero pressure, depending on the weight percent of small particles (Fig. 14.6a). The highest strength was achieved when the weight percent of Ag microparticles was about 80 % in the hybrid paste [109–111]. On the other hand, as mentioned above for Ag nanoparticle pastes, the sintering atmosphere also affected the joint by accelerating the depletion of the dispersant [115, 116]. It was found that the presence of oxygen in the sintering atmosphere played a key role in promoting low-temperature and low-pressure sintering of the hybrid Ag-paste. A clever experimental process was designed to control the flow rate of nitrogen and oxygen. In pure nitrogen, the bonding strength was almost zero. The bonding strength sharply increased with increasing oxygen concentration and then become saturated (Fig. 14.6b). There are number of possible reasons for this behavior. The oxygen may have promoted the decomposition of organics in the paste, or it may have induced the reduction of Ag_2O. Alternatively, oxygen may have assisted the densification of the sintered Ag structure, or it may have accelerated the diffusion of between neighboring Ag atoms. The exact role of oxygen remains unknown. However, it is reasonable to suggest that an oxygen partial pressure is required to achieve high-strength joint in these Ag pastes [117]. Furthermore, in order to enhance the adhesion between the hybrid Ag paste and other nonmetal materials, some polymer particles were added to improve adhesion to an LED chip and to nonmetal substrates. This addition did not reduce conductivity and even improved joint strength [110].

Additionally, the use of a hybrid paste, produced with low-temperature sintering and without applying high pressure, as a die-attachment material was demonstrated

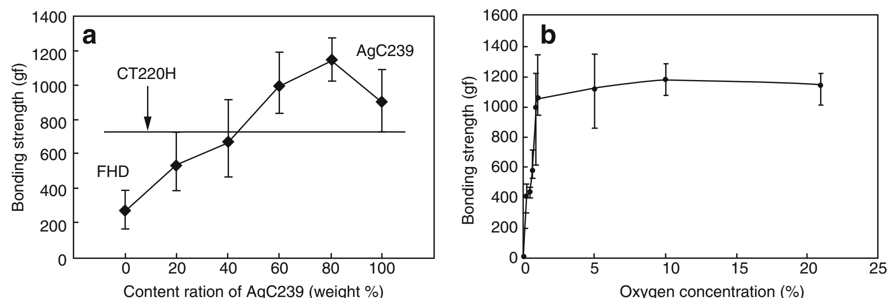

Fig. 14.6 The joint strength depended on the content ratio of micro-Ag (**a**) and oxygen concentrations (**b**) [106]

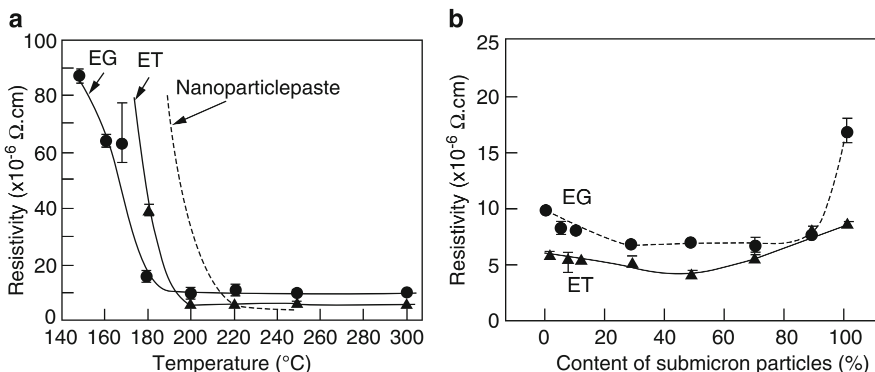

Fig. 14.7 Resistivity change of Ag pastes with sintering temperature (**a**) and content of submicron particles sintered at 200 °C for 30 min (**b**). *EG* ethylene glycol, *ET* ethanol as solvent [111]

[111]. This observation could potentially lead to the widespread use of hybrid Ag pastes instead of traditional solders. For example, the resistivity of hybrid Ag paste exhibited a continuous decrease with sintering temperatures. Above 200 °C, the resistivity decreased to less than 1×10^{-5} Ω.cm, which is equivalent even lower than the values obtained with Ag nanoparticle pastes (Fig. 14.7a). This can be attributed to the reduced level of organic surface residues in the hybrid Ag pastes and excellent package of Ag particles with different size. The resistivity also depended on the level of the addition of submicron Ag particle in the hybrid paste (Fig. 14.7b). The microstructural changes during sintering clearly suggest that a close-packed Ag skeleton structure was formed in the hybrid paste (Fig. 14.8). This contributed to the high shear strength of 31 MPa obtained at 300 °C under a small bonding pressure of 0.4 MPa [111]. Furthermore, it is worth noting that the joint made by the hybrid Ag paste can maintain a high strength of 31 MPa, even after extreme thermal cycles from −40 °C to 300 °C, repeated for 250 cycles.

In contrast, when only Ag microparticles were used as die-attachment materials, the joint strength always decreased rapidly for high-temperature storage times greater than 100 h [118]. The fractures always occurred at the interface between the SiC chip and the silver paste, suggesting that some of the large cracks were formed by the bridging growth of neighboring pores, which occurred due to thermal stress (Fig. 14.9). This might result from a mismatch in the coefficient of thermal expansion (CTE) between the SiC chip and the substrate. Heuck et al. reported a silver paste with an improved CTE, where the paste was composed of micron-sized SiC particles and micron-sized Ag particles; the improved CTE led to improved mechanical stability and electrical resistivity of the joints fabricated with the Ag paste [119]. Nano- and micron-sized silicon carbide particles (SiCp) have also been used as reinforcements in metal matrix composites (MMCs) because of attractive properties such as low density, high hardness, and superior thermal conductivity [120, 121]. Attempts were made to improve the high-temperature stability of Ag

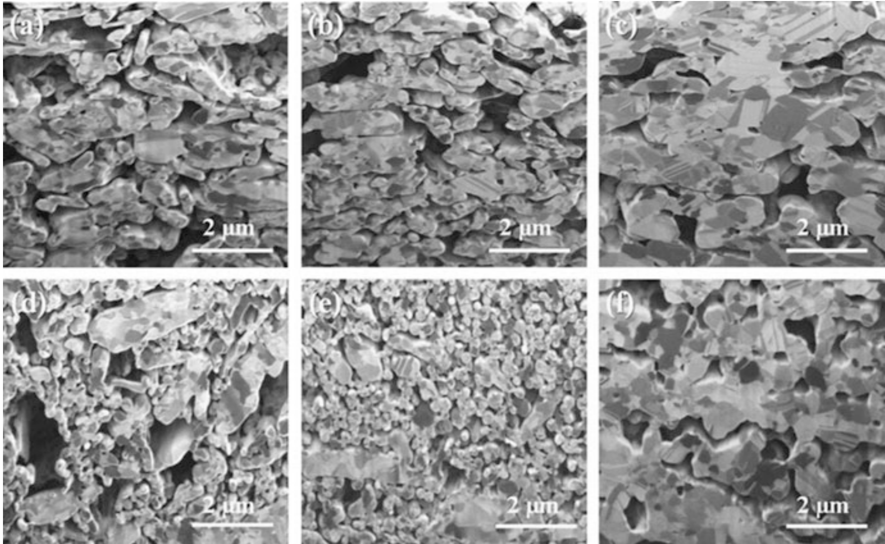

Fig. 14.8 Microstructural changes of the micron Ag and the hybrid Ag pastes in sintering at 200 °C (SIM). All cross sections were obtained from the vertical cut of the Ag tracks. (**a**–**c**) Micron Ag paste, (**d**–**f**) hybrid Ag paste; (**a**, **d**) 5 min, (**b**, **e**) 10 min, and (**c**, **f**) 30 min [111]

microparticle pastes through the addition of SiCp [122]. When appropriate levels of SiCp were added to the Ag microparticle paste, the strength of the joint was not reduced but rather was increased. More importantly, the addition of SiCp greatly improved the high-temperature stability of the joint, to an extent which was dependent on the concentration of SiCp in the Ag paste. SiCp inhibited the growth of grains and pores, which decreased the coarsening of sintering Ag structure under high-temperature operation, in particular at 250 °C, which is the ideal operation temperature for high-power SiC devices. After aging for 500 h, the porous Ag structure formed by this Ag paste mixture was unchanged from the structure that was present after the initial bonding process (Fig. 14.10). The hardness and high-temperature resistance of the SiC particles hindered coarsening of the porous silver [122]. These results encourage further searches for suitable additives and/or new methods that will improve the performance of joints formed by hybrid Ag pastes.

A high joint strength over 40 MPa has also been obtained by designing and optimizing the diameter of Ag particles in hybrid Ag paste, which was then processed at 200 °C with a pressure of only 0.4 MPa [108]. The high strength was the result of a dense Ag structure formed by the uniform and ordered arrangement of Ag particles with an optimized distribution of particle sizes. In particular, the joint strength was maintained, even after storage at 250 °C for over 500 h, in contrast to the performance of an Ag microparticle paste (Fig. 14.11). This excellent high-temperature stability was the result of a condensed and bulk-like bonding interface between chips and substrates, formed during the high-temperature process [123].

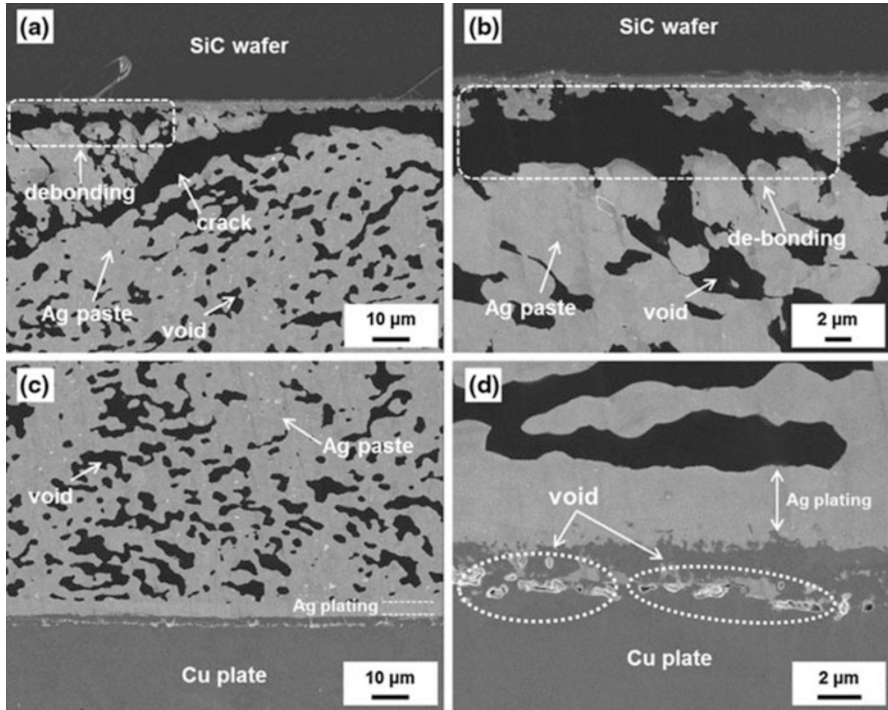

Fig. 14.9 Interfacial microstructures of Ag flake layer in SiC die attachment, damaged by the H-thermal cycles: (**a**) SEM image of SiC wafer side interface, (**b**) higher magnification image of the wafer side, (**c**) Cu plate side image, and (**d**) the high magnification [118]

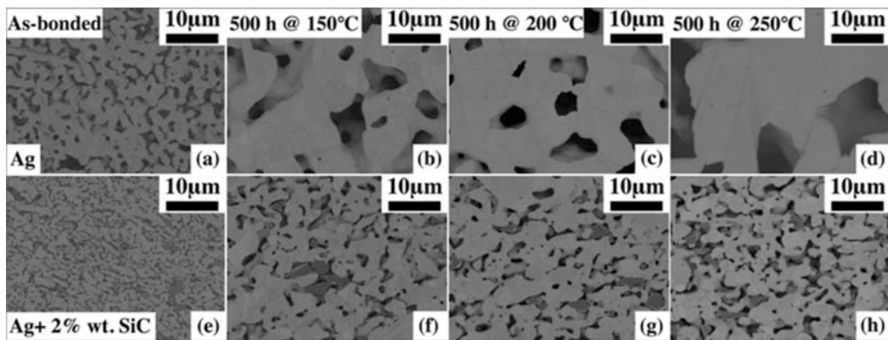

Fig. 14.10 Evolution of cross-sectional morphology after aging at 150, 200, and 250 °C for 500 h: (**a–d**) joints with no additive; (**e**, **f**) joints with added SiC; (**a**) and (**e**) are the as-bonded state [122]

The reliability of joints is affected by the substrate choice, as well as by the size of the Ag particles used in the paste [124]. The thermal and mechanical properties of the paste and the substrate must be matched. Moreover, the solvents in Ag pastes

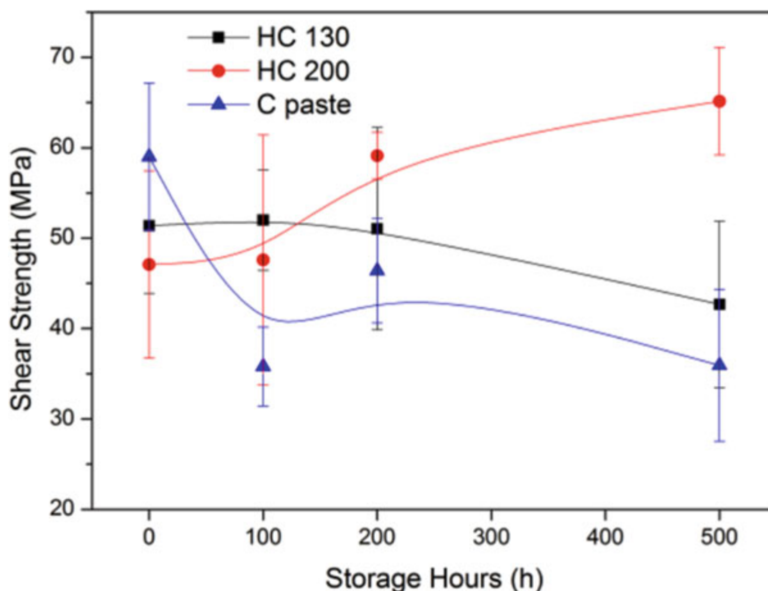

Fig. 14.11 Shear strength of Ag pastes after high-temperature storage at 250 °C. HC130: size distribution from 230 to 900 nm. HC200: size distribution from 280 to 500 nm. C paste: micro-Ag with a size of 8 μm [123]

have important effects on the viscosity, fluidity, reactivity, and sintering behavior of Ag [125–127]. When a solvent with excellent shear thinning behavior was selected to optimize the performance of a hybrid Ag paste, a joint strength greater than 80 MPa was achieved at 280 °C with a small applied pressure [128]. The slow evaporation and decomposition of the solvent contributed to the high strength, because the slow speed of solvent removal allowed densification and shrinkage of the sintered, porous Ag structure. Consideration of the effects of solvent on the sintering behavior of Ag pastes might prove to be a new path to achieving the sintering of such pastes at low temperature and low pressure.

14.3 Copper Pastes

There are many reports of the use of Ag pastes as joining materials because Ag has the highest thermal conductivity among metals, has a high melting point (963 °C), and because Ag particles can be synthesized easily and are chemically stable in air. Moreover, Ag particles remain bond, even at temperatures higher than the melting point of the Ag particles, because the Ag particles convert to a bulk state during bonding. Thus, Ag pastes have the potential to produce joints in power devices that will endure the severe conditions of operation at temperatures greater than 200 °C. Although Ag nanoparticles work well for die-attaching materials, they have some

disadvantages: Ag is relatively expensive, is prone to migration under an applied voltage, and is susceptible to moisture damage, which leads to short device lifetimes. Therefore, it is inevitable that the development of alternative materials has become a goal. Compared to metallic Ag, copper is only 6 % less conductive but it is 1000 times more abundant and 100 times less expensive. More importantly, copper is also robust to electromigration. For these reasons, copper pastes have become ideal alternatives to silver paste and have been studied in recent days [98, 129, 130]. Although copper has many advantages, it is susceptible to oxidation in water or air, because of contact of the Cu particles with oxygen. This drawback limits the overall advantage of metallic Cu pastes [131–134]. This point should be remembered when the cheap Cu pastes are used as die-attaching materials in power devices.

14.3.1 Synthesis of Cu Pastes

In general, the process steps for Cu pastes are similar to those of Ag pastes. The first step is the fabrication of the paste. As for Ag pastes, Cu pastes are composed by micro- or nano-sized Cu particles. There are many methods to make Cu particles, including radiation methods [135], supercritical fluid techniques [136, 137], laser ablation [138], vacuum vapor deposition [139], and chemical reduction [140, 141]. For use in semiconductor assembly, the synthesis of metal particles needs to be cost-effective and have high yields at large scale. Polyol synthesis is a simple, large-scale method of preparing metal nanoparticles by adjusting parameters such as reaction time and temperature and by selecting suitable capping agents and additives [142–145]. The electrical wire evaporation process is also an attractive technique for low-cost nanoparticle fabrication [146–148]. This technique produces nanoparticles with smaller and narrower particle size distributions compared to nanoparticles produced in gas atmospheres, and it avoids the agglomeration and the formation of by-products, which are formed in some more complicated chemical synthetic processes. Both of these large-scale synthetic methods can continuously produce Cu particles with gram level; however, limitations in particle extraction from the reaction medium remain a concern for producing large volumes of metal particles. There are other simple methods to make Cu particles, including the mechanical ball-milling method. Different types of milling machines can be used to prepare micro-sized Cu particles in large volumes; the type of mill, milling speed, temperature, time, atmosphere, and container type are important production parameters [149]. However, the milling method has some limitations, including difficulty in the production of nano- and submicron-sized particles and long production times. Recently, an oxygen combustion method was used to produce metal nanoparticles, in large volumes, in a vacuum environment; however, while large supplies of product could be obtained, a thin oxide layer was always present on the surfaces of the copper particles. Details of synthetic techniques for Cu micro- and nanoparticles can be found in some recent reviews [131, 150–153]. Alternatively,

some Cu compounds have also been used as die-attachment materials. These Cu compounds decompose in situ, during the sintering process, and form Cu particles and bonding [154, 155].

14.3.2 Anti-oxidation Methods for the Sintering of Cu Pastes

Metallic Cu is a promising material for bonding because it is cheap, and electromigration does not take place as readily as it does with metallic Ag. The main problem with Cu particles, even micro-sized particles, is that they are easily oxidized in air. Furthermore, it is difficult to stabilize pure Cu particles that do not have an oxide layer. Even when starting with pure Cu particles that have been prepared under an inert gas environment, the oxidation of Cu particles, which occurs during the heat treatment of Cu pastes, remains a huge challenge for the use of Cu particles in bonds.

The most common method is heat a Cu paste in high vacuum, above 200 °C in a reducing or an inert atmosphere, such as hydrogen or nitrogen [156–162]. The main oxide layer on the surface of Cu particles is CuO and Cu_2O, which can be easily reduced to metallic Cu at a suitable temperature and under atmospheric hydrogen conditions [163]. Normally, CuO reduces directly to metallic Cu without formation of an intermediate or suboxide (i.e., no Cu_4O_3 or Cu_2O) and is easier to be reduced than Cu_2O. Therefore, by controlling the composition of the oxide layer on the surface of Cu particles, it is possible to obtain high performance with sintered Cu structures. Very detailed studies of the sintering of copper powders, using different oxygen levels, and various sintering atmospheres (H_2, 90%N_2-10%H_2, N_2, and vacuum), strongly suggest that the sintering process should be carried out in an atmosphere with low hydrogen content, or in under vacuum, or in an inert gas atmosphere. For example, in order to prevent cracking and swelling during the process of forming the sintered copper structure, copper powders with low oxygen content should be used; this might decrease the formation of water due to the hydrogen–oxygen reaction [164]. On the other hand, Champion et al. found that the reduction temperature of the oxide layer on the surface of Cu nanoparticles, under a sintering atmosphere that contained hydrogen, was lower than that on micron-sized particles or on bulk copper, primarily as a result of the large surface curvature of the nanoparticles [165]. Rathmell et al. reported a transparent film comprised of copper nanowires (CuNWs) with a sheet resistance of about 30 Ω sq^{-1} and a transmittance of 85 %; this film was produced by sintering at only 175 °C in a tube furnace with a pure hydrogen atmosphere, after the film had been cleaned in a gas atmosphere of 5 % hydrogen and 95 % nitrogen at room temperature [156]. The bendable and flexible transparent Cu film could carry a maximum current density of 0.533 A cm^{-2} at a voltage ramp of 1.57 V s^{-1}, compared to 0.866 A cm^{-2} at a voltage ramp of 1.61 V s^{-1} for ITO film (Fig. 14.12). It has also been suggested that even Cu nanoparticles with an oxide layer would benefit from low-temperature sintering.

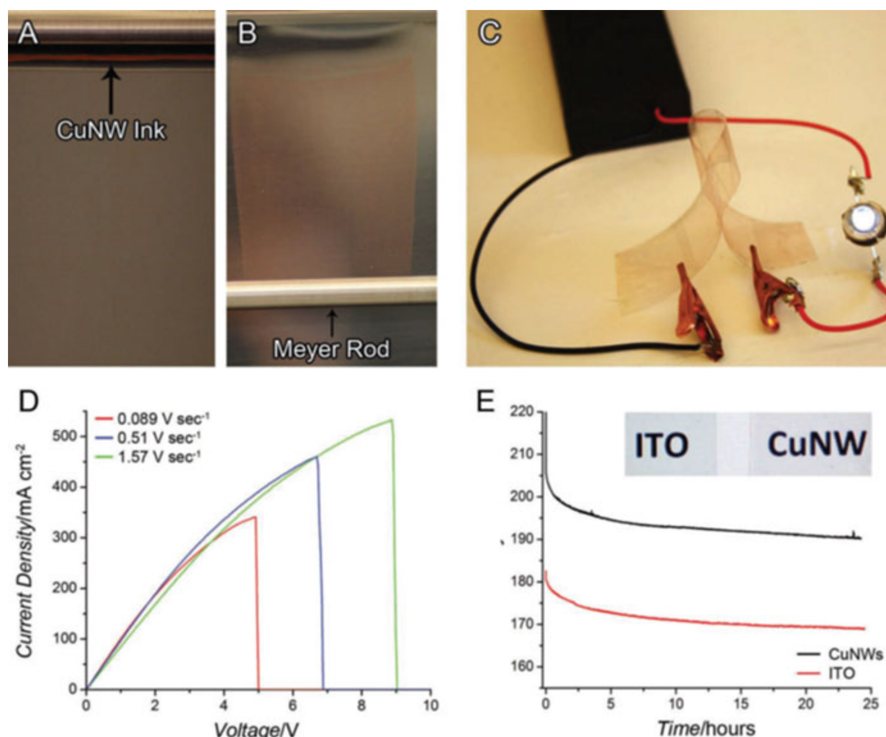

Fig. 14.12 (**a**, **b**) CuNW ink before and after coating on PET with a Mayer rod. (**c**) A bent CuNW film (25 Ω sq^{-1} and 83 % transparent) completing an electrical circuit with a battery pack and an LED. (**d**) Plot of current versus voltage for 40 Ω sq^{-1} CuNW films, demonstrating their maximum current-carrying capacity. (**e**) Current versus time plot for films of CuNWs (40 Ω sq^{-1}) and ITO (42 Ω sq^{-1}) with an applied voltage of 1.5 V over 24 h demonstrates the relative stability of CuNW films over time. The inset of (**e**) shows a visual comparison of ITO (10 Ω sq^{-1}) and CuNW (75 Ω sq^{-1}) films, both 88 % transparent, backlit by an iPhone display [156]

Although the hydrogen plasma is the most widely used and best known method to reduce copper oxide to copper metal, the risks and complexity of this method present serious problems in industrial applications. Recently, some safer non-plasma methods that use reducing agents have been developed for copper oxide reduction. When a thick copper oxide film was exposed to reducing agents (ethanol or formic acid) below 400 °C, using nitrogen as a carrier gas, it was completely reduced to elemental copper in just a few minutes [166]. The process was very simple and fast and was controlled by varying the vapor pressure of the reducing agents. The copper oxide film was completely reduced in 5 min at temperatures below 400 °C. Surprisingly, oxygen was rapidly removed from deep under the copper surface (~400 nm), apparently due to the high mobility of oxygen and its sensitivity for concentration gradients. Ethanol was a slightly better reducing agent than methanol. Formic acid was stronger than alcohol and even reduced copper oxide at temperatures below 310 °C. The reduction temperature could also

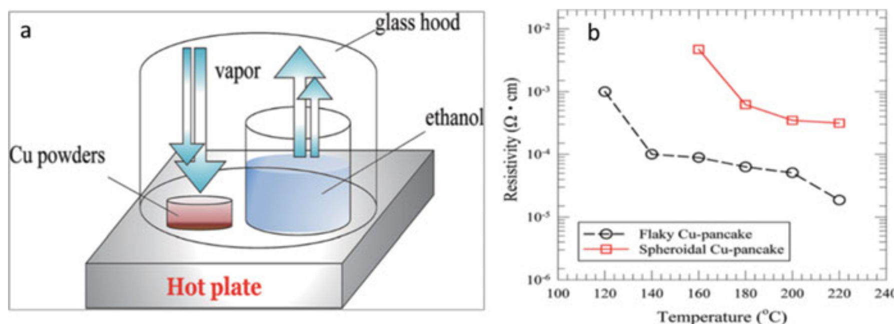

Fig. 14.13 Schematic diagram of the apparatus for ethanol-assisted sintering (**a**) and the electrical resistivity of spheroidal (15 μm) and flaky (50 μm) copper powders after annealing in ethanol vapor at various temperatures (**b**) [169]

be decreased by decreasing the size of the Cu particles. Jang et al. sintered Cu nanoparticles under a formic acid atmosphere, to produce copper patterns at just 250 °C [167]. These Cu nanoparticles, with diameter of 5 nm, grew into large grains, with sizes above 500 nm, achieving Cu patterns with low resistivity. Generally, the oxidation and reduction reactions of copper compete during the sintering process. The copper oxide crystalline domains increase more rapidly when the temperatures are higher than 200 °C. Therefore, at higher temperatures, the rate of oxidation may be greater than the rate of reduction. Furthermore, decreasing the sintering temperature might be favorable for the sintering of copper nanoparticles. Yu et al. obtained highly conductive Cu patterns with a formic acid atmosphere at only 200 °C, which was high enough to allow melting of the surfaces of the 25 nm Cu nanoparticles, creating a conductive network [168]. In order to apply these Cu patterns to polymer substrates with low heat resistance, micron-sized Cu powders were sintered at 120 °C on a hot plate, with the assistant of ethanol vapor, to produce highly conductive Cu patterns (Fig. 14.13). The low sintering temperature was attributed to the reduction of the native oxide on the surfaces of the Cu powders by the ethanol vapor. The Cu particles produced by reduction are very active and tend to sinter with each other to lower the surface energy, producing excellent conductive paths [169]. Compared to hydrogen sintering, sintering with reduction agents is a simple and safe process. By tailoring of size distributions of the Cu particles, the sintering temperature might be decreased further, allowing the widespread use of low-cost Cu pastes in various devices.

The problem of oxidation of Cu particles might also be addressed by minimizing the exposure of the copper particles to oxygen. Some special sintering techniques, which can even be used in air, has been developed to very rapidly anneal Cu particles [132, 170–173]. It is known that intense flashlamp annealing is a millisecond process. This process uses irradiation with visible light with a broad spectral range. During this process, the temperature of the target materials can be instantaneously increased by several hundred degrees, far above the decomposition

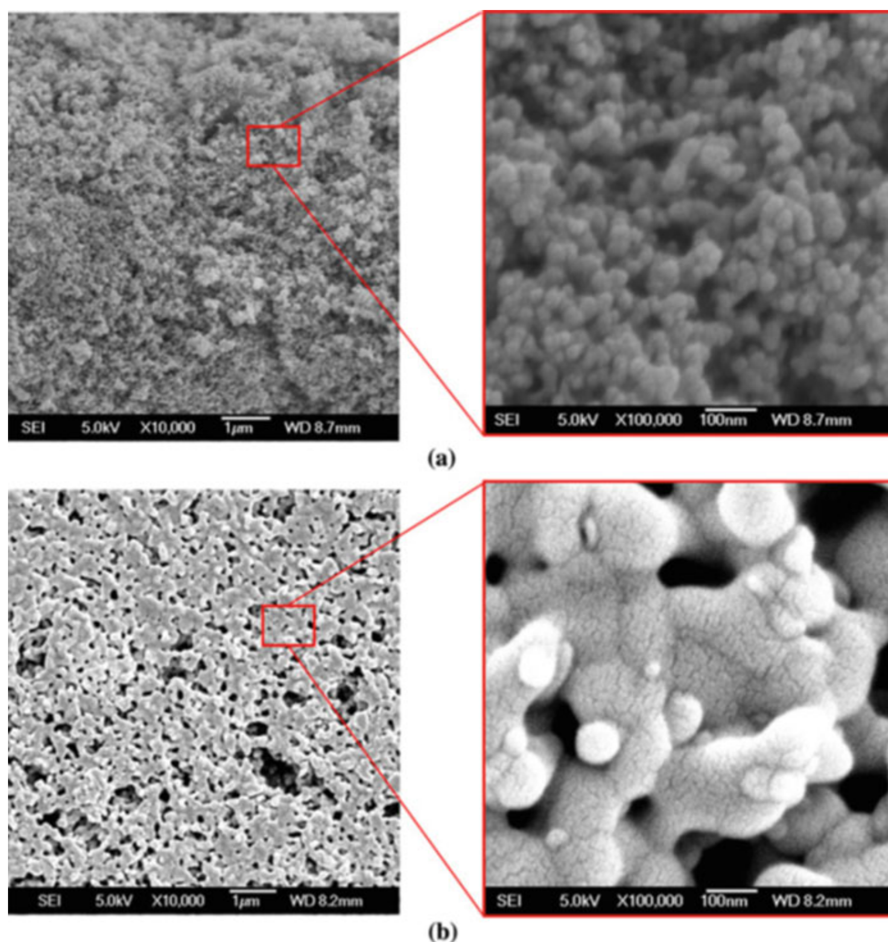

Fig. 14.14 SEM images of copper nanoparticles: (**a**) dry nanoparticles; (**b**) sintered copper nanoparticles after reactive IPL sintering [173]

temperature of copper oxide and organics. Due to the short time at this temperature, the bare Cu particles have no chance to reoxidize; rather, they are sintered together, even in ambient conditions. Cu nanoparticles with an oxide shell were sintered with an intense flashlamp, which successfully removed the oxide shells and produced a conductive, pure copper film in a short period of time (2 ms) under ambient conditions (Fig. 14.14). The in situ copper oxide reduction may correlate with the presence of organic materials, such as polyvinylpyrrolidone (PVP), which decompose to release reducing agents [173]. Joo et al. found that the synergistic interactions between Cu nano-ink (with 20–50 nm diameter particles) and Cu micro-ink (with 2 μm diameter particles) were enhanced during flashlamp sintering, and this contributed to the formation of a dense and pure Cu network structure [170]. The temperature of Cu nano- and micro-ink films increased instantaneously upon

flashlamp irradiation. The maximum temperature reached in Cu nanofilms (about 290 °C) was far higher than in Cu microfilms, because Cu nanoparticles have a higher specific surface area. Thus, Cu nanofilms can absorb light more efficiently than Cu microfilms. Moreover, the temperature of Cu nanofilms stayed constant for some amount of time after the irradiation ended, while the temperature of Cu microfilms began to decrease immediately after the flashlamp irradiation ended. To take advantage of the high-temperature properties of Cu nanofilms, which are exhibited under flash irradiation, organic materials and other impurities present in the hybrid ink (composed of Cu nano- and microparticles) must completely be removed. This will likely produce a highly conductive Cu film that has many of the same benefits and functions exhibited by hybrid Ag pastes.

To reduce oxidation of Cu particles, a protective surface layer, composed of a secondary material, can be added to the Cu particles. Potential secondary materials include carbon-based materials (such as carbon and graphene), surfactants, polymers, silica, and metals [131]. The secondary materials should be stable at low temperature and should decompose, in situ, at high temperature, to avoid the any oxidation of the Cu particles. A thick graphene layer of about 3 nm was coated on the surface of Cu nanoparticles; this layer prevented oxidation at temperatures below 165 °C, even in air [174]. Crystalline Cu cores, completely surrounded with a thin carbon layer with a thickness of about 1 nm, were heated at 200 °C for about 10 min to yield an oxide-free copper network structure with an electrical resistivity of 25.1 μΩ cm in air [175]. The nanoparticles showed high thermal stability against oxidation up to about 180 °C (Fig. 14.15). Cu nanoparticles coated with PVP also can effectively prevent the oxidation of Cu when heated in air [176]. A robust bonding of Cu wires to Cu pads was realized with the PVP-coated Cu nanoparticles, at the low temperature of 170 °C, even in air. It is known that Cu nanoparticles are very difficult to store due to oxidation by the ambient atmosphere. A recent report suggests that the PVP-capped Cu nanoparticles, dispersed in alcohol, had good long-term stability. This was attributed to the uniform and orderly arrangement of PVP polymer chains, with large

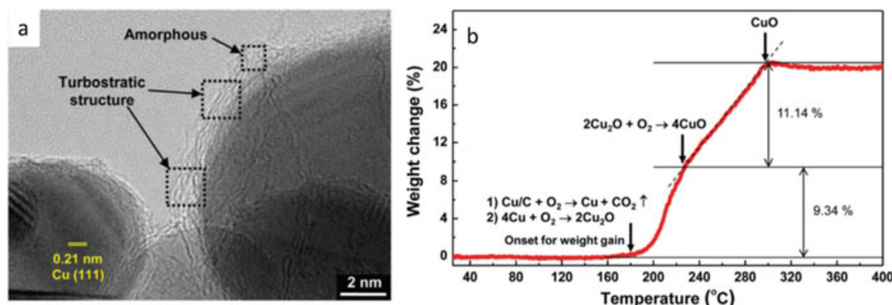

Fig. 14.15 (**a**) Representative high-magnification TEM image of the core–shell Cu-C nanostructure and (**b**) a typical TG curve of the Cu–C NPs oxidized in air [175]

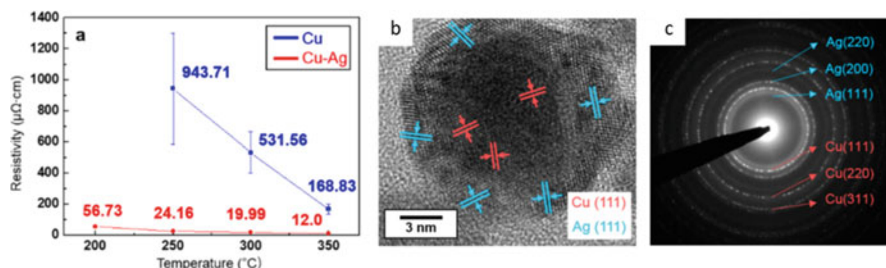

Fig. 14.16 Electrical resistivity of the Cu conductive ink (*blue line*) and of the Cu–Ag conductive ink (*red line*) under a N2 gas atmosphere (**a**), HRTEM image of a Cu–Ag nanoparticle (**b**), and SAED pattern of the nanoparticles (**c**) [177]

radii of gyration and coil-like conformations, on the surfaces of Cu nanoparticles. These arrangements provided protection against dissolved oxygen [137].

It is clear that the suitable coating agents for the surfaces of Cu nanoparticles are needed. Core–shell structures offer an effective method avoiding oxidation of Cu particles. Uniform Cu–Ag, core–shell nanoparticles, synthesized by a two-step process of thermal decomposition and galvanic displacement, can be sintered up to 350 °C in a nitrogen atmosphere without any oxidation [177]. The resistivity of the Cu core–Ag shell nanoparticles, sintered as low as 200 °C, was only 56.73 μΩ cm, which is sufficiently low to prevent damage to flexible substrates. The high conductivity of these materials is attributed to the complete surface coverage of the Cu nanoparticle by the Ag shell (Fig. 14.16). Other shell materials, such as Sn [178] and NiO [179], have been used to prevent the oxidation of Cu particles in storage or during the sintering process. All of the methods mentioned above can slow down the oxidation of Cu particles to some extent, but they cannot completely prevent the oxidation process. The development of new strategies is still required to enable the widespread application of low-cost Cu particles in advanced devices.

14.3.3 The Joint Performance of Cu Pastes

Sintered Ag pastes, with their excellent thermal, electrical, and mechanical properties, have long been promising die-attachment materials for electronic modules that demand high thermal and mechanical stability and met most user requirements. One disadvantage of Ag sintering is that successful die attachment requires an oxide-free, noble metal finish of the bonding partners to increase the poor resistance of Ag to electromigration. Direct bonded copper (DBC) substrates, which are extensively used as substrates for power electronics, need to be metalized, e.g., silver plated, Ni–Au plated, or Ni–Ag plated, and this increases the cost and complexity of production. It reduces the attractiveness of silver pastes as die-attached materials. Copper paste is a very promising, low-cost alternative to silver paste. Copper offers very good mechanical robustness because it has a lower

coefficient of thermal expansion (CTE) than silver and very high electrical and thermal conductivities. Given the higher cost of Ag and the need for metallization of DBC substrates to prevent silver electromigration in power devices, Cu pastes have been used as die-attachment materials in recent years.

As mentioned above, the oxidation of copper in air inhibits Cu sintering. However, many techniques have been proposed to sinter Cu paste for die attachments, including sintering under high vacuum and under H_2 or N_2 atmospheres. Krishnan reported a cost-effective method to produce Cu nanoparticles using pulsed wire evaporation in deionized water [148]. These Cu nanoparticles were not mixed with any precursor or organic binder system; this led to oxidization almost immediately after synthesis. The nanoparticles were reduced under a forming gas mixture of $95\%N_2$–$5\%H_2$ and used to bond two Cu substrates at 350 and 400 °C. A bonding pressure of 10 MPa at 400 °C gave the highest shear strength. Similar to the sintering process of Ag paste, the parameters of sintering temperature, pressure, and time, particle morphology and size, and composition of the Cu paste strongly affected the joint strength. The shear strength of the Cu joint was increased from about 5 MPa at 280 °C to over 30 MPa at 400 °C when a Cu paste with nanoparticles of about 10–20 nm in diameter were heated under a jointing pressure of 15 MPa in a nitrogen atmosphere [129]. Moreover, the addition of a preheat step also affected the joint strength. High preheat temperatures decreased the joint strength of the Cu joint as a result of the gradual sintering and growth of nanoparticles during the preheat step and the subsequent inhibition of diffusion growth in the second heating step [129]. This was also seen in the Ag sintering process. High purity Cu nanoparticles capped with fatty acids and amines were synthesized from inexpensive raw materials, in ethylene glycol, with high yield [162]. The mean diameter of the Cu nanoparticles was controlled from 93 to 13 nm, as the alkyl carbon number increased from C10 to C22 (Fig. 14.17). These Cu nanoparticles were used to bond Cu substrates with a two-step heating process: 10 min at 150 °C, followed at second temperature for 5 min, under a bonding pressure of 5 MPa. The shear strength increased with the sintering temperature and depended on the size of Cu nanoparticles (Fig. 14.17). The low sintering temperature and small particle size resulted in high joint strength. These benefits could be

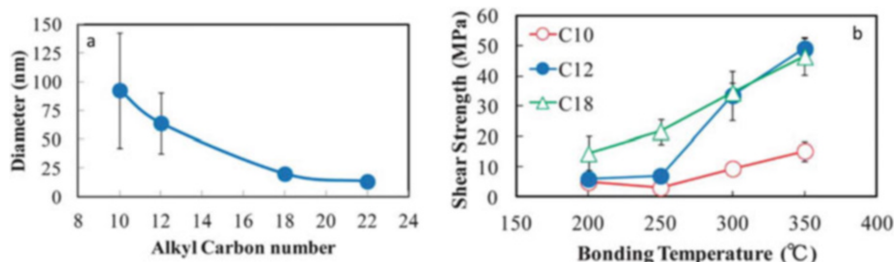

Fig. 14.17 Mean diameters of the Cu nanoparticles capped by fatty acid and fatty amine by increasing the alkyl carbon number from C10 to C22 (**a**) and shear strengths of the Cu plates bonded by the C10–C18 Cu nanoparticles (**b**) [162]

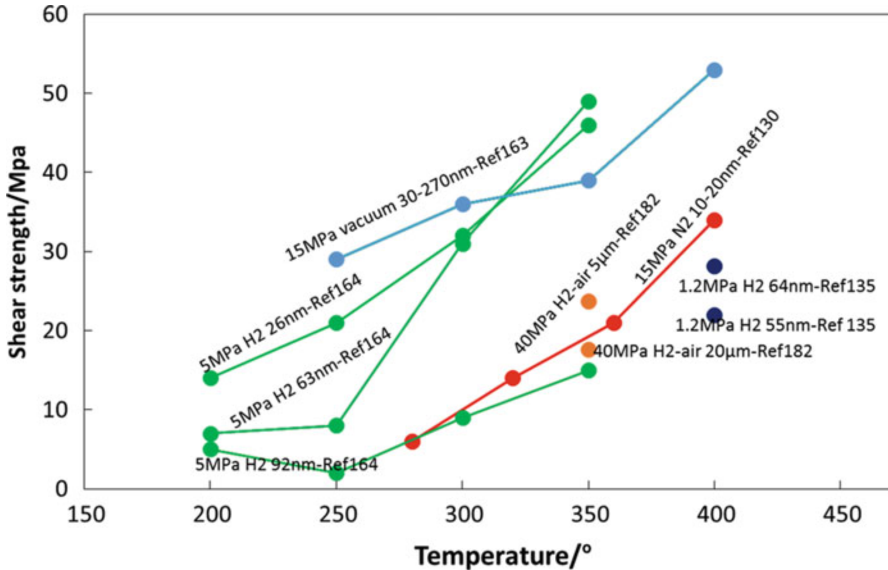

Fig. 14.18 Effect of the bonding pressure and temperature on shear strength of Cu pastes joints under various atmospheres with different bonding times [129, 134, 161, 162, 180]

attributed to the ease of sintering of small nanoparticles and the resulting dense structure. The shear strength of the Cu joints was over 30 MPa, the same shear strength as for Ag pastes, and this has greatly encouraged further development of Cu nanopastes.

In order to reduce processing costs, and to take advantage of other beneficial properties of Cu materials, a novel sintering process for micron-sized Cu powders was developed [180]. The Cu powders were pretreated in a H_2 atmosphere to remove the oxide layer from the surface of the Cu particles, producing pure, oxide-free particles. Subsequently, the Cu powders were sintered for only a few minutes in air, at a pressure of 40 MPa and a temperature of 350 °C; this produced joints with shear strengths above 20 MPa. The influences of bonding parameters and Cu paste composition on the shear strength were collated and are illustrated in Fig. 14.18. The shear strength depended on sintering temperature and pressure; high temperature and high pressure gave high shear strengths when other sintering conditions and Cu composition were held constant. However, the shear strength also depended on the size of the Cu particles. There was no strong relationship between small particle size and high strength; particle size and distribution of particles are likely key factors in the performance-related properties of Cu pastes.

In order to decrease the oxidation of Cu pastes during the bonding process, Cu pastes with other metal or metal oxide additives, which can slow down the oxidation, have been used to bond Cu plates [181–185]. For these pastes, this sintering process was carried out in H_2 or other reducing atmospheres or in air. For example, NiO particles were mixed with Cu nanoparticles and the mixture was used to bond

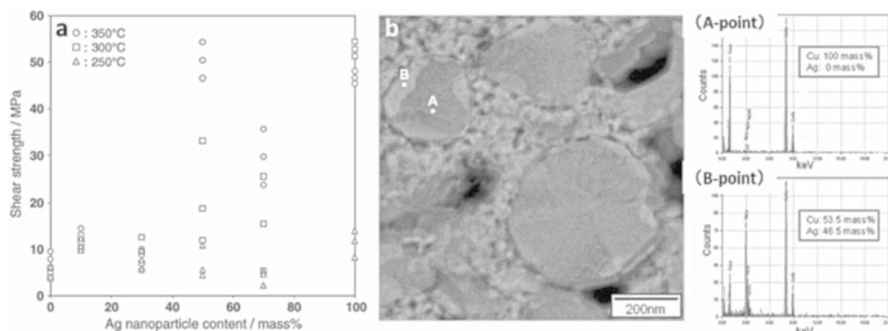

Fig. 14.19 Shear strength of the various Cu-to-Cu joints (**a**) and S-TEM image and EDS spectrums of the mixed Cu–Ag nanoparticle sintered layer formed at 350 °C [98]

Cu plates; shear strengths above 20 MPa were achieved, even with pressure-free bonding condition. A NiO–CuO solid solution was formed in the beginning of the sintering process, and this might contribute to the enhanced strength. The Ni in the bonding layer segregated at the surface and at grain boundaries of crystalline Cu particles, forming a metallic Cu–Ni alloy. These results suggest that NiO addition causes enhanced sintering by surface diffusion in the bonding layer. The increase in surface diffusion results from removal of surface oxides from the Cu nanoparticles during their reaction with the NiO nanoparticles [182]. Strong joints using Cu nanoparticles and enhanced Cu-to-Cu bonding were achieved through the addition of Ag nanoparticles [98]. The paste mixture was preheated at 150 °C for 5 min without pressure and then bonded at a fixed temperature for 5 min under 10 MPa pressure. The joint strength depended on the Ag content in the paste and on the sintering temperature (Fig. 14.19). Above 250 °C, the pastes with Ag levels greater than 50 % achieved higher strength than pure Ag pastes. A solid solution of Ag and Cu at the bonding interface may contribute to the increased strength. Generally, in the case of bulk metals, the solubility limit of Ag in Cu, and Cu in Ag, at room temperature is less than 1 mass%. In the joint, the Ag content in the Cu nanoparticles was 46.5 mass%, which may relate to the high activity of Ag and Cu nanoparticles (Fig. 14.19). Moreover, an Ag–Cu nanopaste was also produced by mixing commercial Ag and Cu nanoparticles with solvent and binder; these mixtures could then be sintered in air at 380 °C, without applying external pressure [183]. The Ag–Cu pastes, with a thick coating layer of binder, were protected from oxidation and achieved high conductivities, even after sintering in air (Fig. 14.20). This also provided a strategy for Cu paste as die attachment.

In other studies, reducing agents were used as solvents, and this assisted in the sintering of Cu particles. For example, pastes composed of micron-sized Cu flake were used to produce Cu-to-Cu joints under a formic acid atmosphere [186]. The shear strength of these joints exceeded 15 MPa, when for processed at 300 °C for 60 min, with a low pressure of 0.4 MPa. The decomposition of the polyethylene glycol (PEG) solvent enhanced the sintering of Cu microparticles by removing the oxidation. To develop suitable reducing solvent is also a promising strategy for Cu paste.

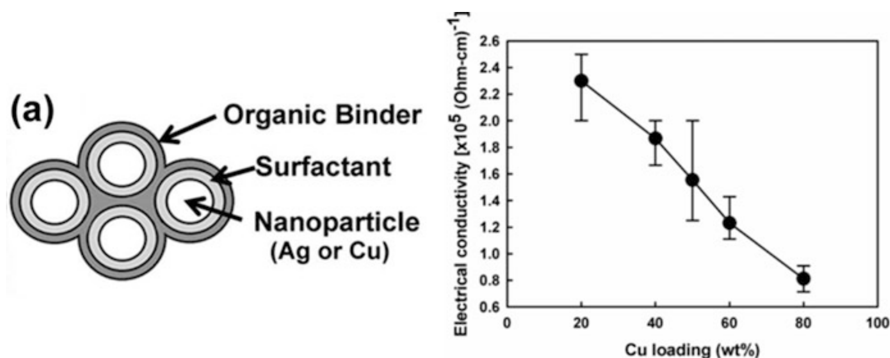

Fig. 14.20 Schematic of organic binder linked up the nanoparticles with surfactant coating (**a**) and electrical conductivity of Ag–Cu nanopaste with various Cu loadings (**b**) [183]

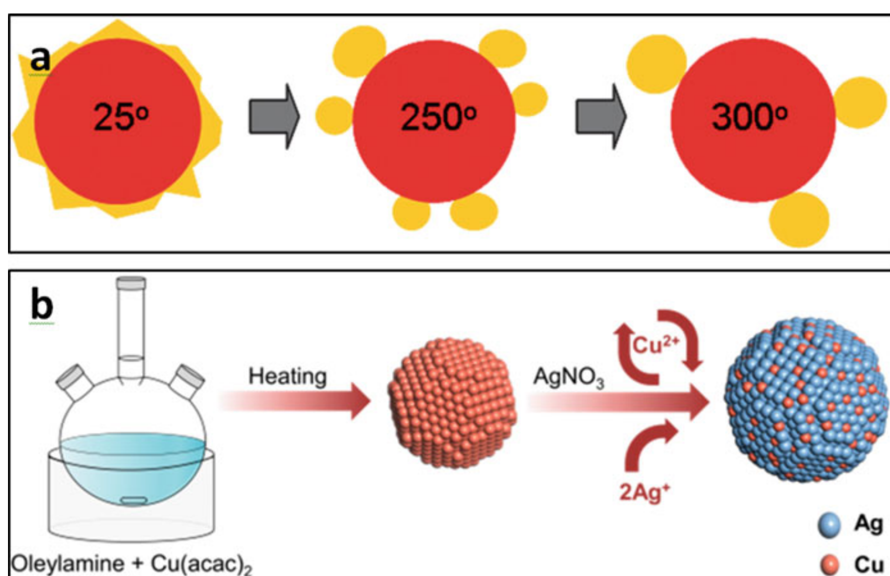

Fig. 14.21 Schematic illustration of the growing silver crystallites from the shell (**a**) [187] and the synthesis of Ag–Cu nanoparticles (**b**) [190]

Furthermore, to avoid the oxidation of low-cost Cu nanoparticles in air, some Cu nanoparticles have been developed where the cores are comprised of Cu and the shells are comprised of other metals. One problem with these particles is that the metal shells tend to aggregate and transform into small particles; these attach to the surface of copper cores when the temperature is raised (Fig. 14.21). These resulting Cu particles are no longer coated by a metal shell. Therefore, if they are exposed to oxygen at this elevated temperature, they can undergo oxidation, as was indeed found, while heating in air [187, 188]. Therefore, the idea of alloying other metals

with Cu has been proposed [189, 190]. The calculated trends for O_2 adsorption on these Ag–Cu nanoparticles show that the adsorption energy declines rapidly in an O_2 atmosphere. Electron transfer from Cu to Ag within the structure provides far better resistance to oxidation than monometallic Cu nanoparticles, making these materials suitable for use in die-attachment materials.

The high-temperature stability and reliability of Cu joints are seldom studies due to the oxidation in air. With the development of Cu pastes that can potentially substitute for Ag pastes, the reliability of Cu joints becomes an issue. Ishizaki et al. have attempted to evaluate the thermal resistance of Cu nanoparticles joints and found that the joints remained stable, even after 3000 thermal test cycles between 60 and 200 °C [191]. This suggests that Cu joints have excellent thermal resistance; however, the evolution of the Cu structure and the fatigue mechanisms of the Cu joints under real service conditions are still unknown. These questions should be the focus of future studies.

14.4 Other Bonding Techniques

Besides the sintering of metal paste, there are other techniques that can make joints by directly bonding two metal films together, e.g., the "silver direct-bonding" technique. In this technique, diffusion growth of Ag at the bonding interface, due to stress in the Ag film, produces bonding between chip and substrates. The Ag films are generally produced by deposition, either by electrolytic plating or by sputtering methods, on the chip, on the substrates, or on both surfaces. Then the Ag film surfaces are brought together at elevated bonding temperatures, with [192, 193] or without pressure [194–197]. Although stress migration and the resulting stress relaxation at the bonding temperature play a key role in the bonding process, the function of the solvent used in the bonding process, and the role played by the growth of hillocks, remain unclear. Similarly, Cu–Cu direct-bonding techniques have been used for die attachments. Due to the oxidization of Cu, these Cu films need to be activated and brought together under an ultrahigh vacuum condition [198–201]. Bonding pressure or temperature can be optimized to improve joint production. However, the development of simple Cu–Cu direct-bonding methods that can be applied in air may be challenging. Nevertheless, direct-bonding techniques have generated novel opportunities to produce WBG devices at low temperature, low pressure, and large scale.

14.5 Conclusion

This chapter has summarized advanced bonding technologies based on nano- and micro-metal pastes, including those composed of Ag and Cu particles. The influence of sintering parameters on the quality of sintered metal joints was discussed in

detail. Low-temperature and low-pressure (even no pressure) sintering processes have been developed, thanks to the miniaturization of particles and the optimization of particle combinations in these metal pastes. Ag paste has a long history of development and much data on the long-term mechanical properties of Ag joints has been accumulated, in large part because Ag metal particles are easily processed in air. The poor electromigration resistance of Ag joints has stimulated the development of Cu pastes; however, these suffer from the huge problem of oxidation in air. Various measures have been proposed to reduce or eliminate this oxidation; however, further studies are under way. In order to use these low-cost Cu pastes in real devices, future work must address factors such as the design of Cu particles, the composition of Cu pastes, the use of reducing agents, and the use of new sintering processes which would decrease exposure to air. Furthermore, with the development of flexible devices, where the use of metal joints will be common, low-temperature (even room temperature) and zero-pressure bonding processes will be required in the near future.

Acknowledgments This work was partly supported by the COI Stream Project, Grant-in-Aid for Scientific Research (Kaken S, 24226017), and International Research Promotion Program (IRPR) of Osaka University.

References

1. Rupp R, Miesner C, Zverev I (2001) Combination of new generation CoolMOS and thinQ! Silicon Carbide Schottky diodes: new horizons in hard switching applications. In: Proceedings of the 2001 power conversion intelligent motion conference (PCIM 2001), Chicago, 2001
2. Shenai K, Dudley M, Davis RF (2013) Current status and emerging trends in wide bandgap (WBG) semiconductor power switching devices. ECS J Solid State Sci Technol 2:N3055–N3063
3. Millan J (2012) A review of WBG power semiconductor devices. In: Proceedings of the 2012 international semiconductor conference (CAS), vol 1, pp 57–66
4. Ryu S, Hull B, Dhar S et al (2010) Performance, reliability, and robustness of 4H-SiC power DMOSFETs. Mater Sci Forum 645–648:969–974
5. Buttay C, Planson D, Allard B et al (2011) State of the art of high temperature power electronics. Mater Sci Eng B 176:283–288
6. Li J, Johnson CM, Buttay C et al (2015) Bonding strength of multiple SiC die attachment prepared by sintering of Ag nanoparticles. J Mater Process Technol 215:299–308
7. Millan J, Godignon P, Perpina X et al (2014) A survey of wide bandgap power semiconductor devices. IEEE Trans Power Electron 29:2155–2163
8. Suganuma K, Nagao S, Sugahara T et al (2015) Silver sinter joining and stress migration bonding for WBG die-attach. ECS Trans 69:21–26
9. Johnson RW, Evans JL, Jacobsen P et al (2004) The changing automotive environment: high-temperature electronics. IEEE Trans Electron Packag Manuf 27:164–176
10. Godignon P, Jorda X, Vellvehi M et al (2011) SiC Schottky diodes for harsh environment space applications. IEEE Trans Ind Electron 58:2582–2590
11. Nah JW, Paik KW, Suh JO et al (2003) Electromigration in flip chip solder joints having a thick Cu column bump and a shallow solder interconnect. J Appl Phys 94:7560–7566

12. Tu KN, Zeng K (2001) Tin–lead (SnPb) solder reaction in flip chip technology. Mater Sci Eng R 34:1–58
13. Chen C, Wang K, Chen K (2007) Isothermal solid-state aging of Pb-5Sn solder bump on Ni/Cu/Ti under bump metallization. J Alloys Compd 432:122–128
14. Jang JW, Hayes S, Lin JK et al (2004) Interfacial reaction of eutectic AuSi solder with Si (100). J Appl Phys 95:6077–6081
15. Kim SJ, Kim KS, Suganuma K et al (2009) Interfacial reaction of Si die-attachment with Zn-Sn and Au-20Sn high temperature lead-free solders on Cu substrates. J Electron Mater 38:872–883
16. Chidambaram V, Hald J, Hattel J (2010) Development of Au-Ge based candidate as an alternative to high-lead content solders. J Alloys Compd 490:170–179
17. Yoon JW, Noh BI, Jung SB (2011) Interfacial reaction between Au-Sn solder and Au/Ni-metallized kovar. J Mater Sci Mater Electron 22:84–90
18. Song JM, Chuang HY, Wu ZW (2006) Interfacial reactions between Bi-Ag high-temperature solders and metallic substrates. J Electron Mater 35:1041–1049
19. Song JM, Chuang HY, Wen TX (2007) Thermal and tensile properties of Bi-Ag alloys. Metall Mater Trans A 38:1371–1375
20. Shimizu T, Ishikawa H, Ohnuma I et al (1999) Zn-Al-Mg-Ga alloys as Pb-free solder for die-attaching use. J Electron Mater 28:1172–1175
21. Kang N, Na HS, Kim SJ et al (2009) Alloy design of Zn-Al-Cu solder for ultra-high temperatures. J Alloys Compd 467:246–250
22. Haque A, Lim BH, Haseeb ASMA et al (2012) Die attach properties of Zn-Al-Mg-Ga based high-temperature lead-free solder on Cu lead-frame. J Mater Sci Mater Electron 23:115–123
23. Lee JE, Kim KS, Suganuma K et al (2005) Interfacial properties of Zn-Sn alloys as high temperature lead-free solder on Cu substrate. Mater Trans 46:2413–2418
24. Park SW, Sugahara T, Kim KS et al (2012) Enhanced ductility and oxidation resistance of Zn through the addition of minor elements for use in wide-gap semiconductor die-bonding materials. J Alloys Compd 542:236–240
25. Park SW, Nagao S, Sugahara T et al (2013) Retarding intermetallic compounds growth of Zn high-temperature solder and Cu substrate by trace element addition. J Mater Sci Mater Electron 24:4704–4712
26. Lee JE, Kim KS, Suganuma K et al (2007) Thermal properties and phase stability of Zn-Sn and Zn-In alloys as high temperature lead-free solder. Mater Trans 48:584–593
27. Chidambaram V, Hattel J, Hald J (2011) High-temperature lead-free solder alternatives. Microelectron Eng 88:981–989
28. Li M, Li Z, Xao Y et al (2013) Rapid formation of Cu/Cu3Sn/Cu joints using ultrasonic bonding process at ambient temperature. Appl Phys Lett 102:094104
29. Li JF, Agyakwa PA, Johnson CM (2011) Interfacial reaction in Cu/Sn/Cu system during the transient liquid phase soldering process. Acta Mater 59:1198–1211
30. Zhang Z, Li M, Wang C (2013) Fabrication of Cu6Sn5 single-crystal layer for under-bump metallization in flip-chip packaging. Intermetallics 42:52–55
31. Park MS, Gibbons SL, Arroyave R (2012) Phase-field simulations of intermetallic compound growth in Cu/Sn/Cu sandwich structure under transient liquid phase bonding conditions. Acta Mater 60:6278–6287
32. Jeong M, Kim J, Kwak B (2012) Effects of annealing and current stressing on the intermetallic compounds growth kinetics of Cu/thin Sn/Cu bump. Microelectron Eng 89:50–54
33. Chuang HY, Yu JJ, Kuo MS et al (2012) Elimination of voids in reactions between Ni and Sn: a novel effect of silver. Scr Mater 66:171–174
34. Siow KS (2012) Mechanical properties of nano-silver joints as die attach materials. J Alloys Compd 514:6–19
35. Siow KS (2014) Are sintered silver joints ready for use as interconnect material in microelectronic packaging? J Electron Mater 43:947–961

36. Peng P, Hu A, Gerlich AP et al (2015) Joining of silver nanomaterials at low temperatures: processes, properties, and applications. ACS Appl Mater Interfaces 7:12597–12618
37. Zhou Y, Hu A (2011) From microjoining to nanojoining. Open Surf Sci J 3:32–41
38. Khazaka R, Mendizabal L, Henry D (2014) Review on joint shear strength of nano-silver paste and its long-term high temperature reliability. J Electron Mater 43:2459–2466
39. Schwarzbauer H (1989) Method of securing electronic components to a substrate. US4810672, Siemens, 1989
40. Schwarzbauer H, Kuhnert R (1991) Novel large area joining technique for improved power device performance. IEEE Trans Ind Appl 27:93–95
41. Ide E, Morita T, Yasuda Y (2006) US2010/0195292A1, Hitachi Ltd, 2010
42. Rasiah IJ (2006) US7083850B2, Honeywell International Inc., 2006
43. Kajiwara R, Motowaki S, Ito K et al (2010) US2010/0195292A1, Renesas Technology Corp, 2010
44. Buttay C, Masson A, Li j et al (2011) Die attach of power devices using silver sintering-bonding process optimization and characterization. IMAPS. High Temperature Electronics Network (HiTEN). Oxford, 2011
45. Frear D, Vianco P (1994) Intermetallic growth and mechanical behavior of low and high melting temperature solder alloys. Metall Mater Trans A 25:1509–1523
46. Abtew M, Selvaduray G (2000) Lead-free solders in microelectronics. Mater Sci Eng 27:95–141
47. Tu K, Gusak A, Li M (2003) Physics and materials challenges for lead-free solders. J Appl Phys 93:1335–1353
48. Li Y, Moon KS, Wong CP (2005) Electronics without lead. Science 308:1419–1420
49. Suganuma K, Kim SJ, Kim KS (2009) High-temperature lead-free solders: properties and possibilities. JOM 61:64–71
50. Goldstem AN, Esher CM, Alivisatos AP (1992) Melting in semiconductor nanocrystals. Science 256:1425–1427
51. Allen GL, Bayles RA, Gile WW, Jesser WA (1986) Small particle melting of pure metals. Thin Solid Films 144:297–308
52. Couchman PR, Jesser WA (1977) Thermodynamic theory of size dependence of melting temperature in metals. Nature 269:481–483
53. Takagi M (1954) Electron-diffraction study of liquid-solid transition of thin metal films. J Phys Soc Jpn 9:359–363
54. Uenishi K, Kawaguchi H, Kobayashi KF (1994) Microstructure of mechanically alloyed Al-In alloys. J Mater Sci 29:4860–4865
55. Zhang M, Efremov MY, Schiettekatte F et al (2000) Size-dependent melting point depression of nanostructures: nanocalorimetric measurements. Phys Rev B 62:10548–10557
56. Ahmadi TS, Wang AL, Grenn TC et al (1998) Shape-controlled synthesis of colloidal platinum nanoparticles. Science 272:1924–1926
57. Morales AM, Lieber CM (1998) A laser ablation method for the synthesis of crystalline semiconductor nanowires. Science 279:208–211
58. Puntes F, Krishnan KM, Alivisatos AP (2001) Colloidal nanocrystal shape and size control: the case of cobalt. Science 291:21152117
59. Boal AK, Iihan F, DeRouchey JE et al (2000) Self-assembly of nanoparticles into structured spherical and network aggregates. Nature 404:746–748
60. Chhowalla M, Amaratunga GAJ (2000) Thin films of fullerene-like MoS2 nanoparticles with ultra-low friction and wear. Nature 407:164–167
61. Sasaki S, Nakamura K, Hamabe Y et al (2001) Production of iron nanoparticles by laser irradiation in a simulation of lunar-like space weathering. Nature 410:555–557
62. Sun Y, Xia Y (2002) Shape-controlled synthesis of gold and silver nanoparticles. Science 298:1276–1279
63. Kirchweger G (2002) Nanoparticles: the next big thing? Mol Ther 6:301–302

64. Rabani E, Reichamn DR, Geissler PL et al (2003) Drying-mediated self-assembly of nanoparticles. Nature 426:271–274
65. Thornton G (2003) Watching nanoparticles grow. Science 300:1378–1379
66. Liz-marzan LM (2006) Tailoring surface Plasmons through the morphology and assembly of metal nanoparticles. Langmuir 22:32–41
67. Mulvaney P, Liz-Marzan LM (2003) Rational materials design using Au core-shell nanocrystals. Top Curr Chem 226:225–246
68. Tang Z, Kotov NA (2005) One-dimensional assemblies of nanoparticles: preparation, properties, and promise. Adv Mater 17:951–962
69. Horn D, Rieger J (2001) Organic nanoparticles in the aqueous phase-theory experiment, and use. Angew Chem Int Ed 40:4330–4361
70. Chen G, Yu L, Mei Y et al (2014) Uniaxial ratcheting behavior of sintered nanosilver joint for electronic packaging. Mater Sci Eng A 591:121–129
71. Li X, Chen G, Wang L et al (2013) Creep properties of low-temperature sintered nano-silver lap shear joints. Mater Sci Eng A 579:108–113
72. Chen G, Zhang ZS, Mei YH et al (2013) Ratcheting behavior of sandwiched assembly joined by sintered nanosilver for power electronics packaging. Microelectron Reliab 53:645–651
73. Li X, Chen G, Chen X, Lu GQ et al (2013) High temperature ratcheting behavior of nano-silver paste sintered lap shear joint under cyclic shear force. Microelectron Reliab 53:174–181
74. Moon K, Dong H, Maric R et al (2005) Thermal behavior of silver nanoparticles for low-temperature interconnect applications. J Electron Mater 34:168–175
75. Huang C, Becker MF, Keto JW et al (2007) Annealing of nanostructured silver films produced by supersonic deposition of nanoparticles. J Appl Phys 102:054308
76. Wang T, Chen X, Lu GO et al (2007) Low-temperature sintering with nano-Silver paste in die-attached interconnection. J Electron Mater 36:1333–1340
77. Joo S, Baldwin DF (2008) Interfacial adhesion of nano-particle silver interconnects for electronics packaging application. In: 58th electronic components and technology conference, ECTC 2008, Lake Buena Vista, 2008, pp 1417–1423
78. Jakubowsk M, Jarosz M, Kiełbasinski K et al (2011) New conductive thick-film paste based on silver nanopowder for high power and high temperature applications. Microelectron Reliab 51:1235–1240
79. Murray AJ, Jaroenapibal P, Koene B, Evoy D (2006) Sintering of silver nanoparticles for the formation of high temperature interconnect joints. Mater Res Soc Symp Proc 942:39–44
80. Tobita M, Yasuda Y, Ide E et al (2010) Optimal design of coating material for nanoparticles and its application for low-temperature interconnection. J Nanopart Res 12:2135–2144
81. Wang S, Li M, Ji M, Wang C (2013) Rapid pressureless low-temperature sintering of Ag nanoparticles for high-power density electronic packaging. Scr Mater 69:789–792
82. Bai JG, Zhang ZZ, Calata JN, Lu GO (2006) Low-temperature sintered nanoscale silver as a novel, semiconductor device-metallized substrate interconnect materials. IEEE Trans Compon Packag Technol 29:589–593
83. Chen X, Li R, Qi K et al (2008) Tensile behavior and ratcheting effect of partially sintered chip-attachment films of a nanoscale silver paste. J Electron Mater 37:1574–1579
84. Yu D, Chen X, Chen G et al (2009) Applying anand model to low-temperature sintered nanoscale silver paste chip attachment. Mater Des 30:4574–4579
85. Mei Y, Lu GO, Chen X et al (2011) Investigation of post-etch copper residue on direct bonded copper (DBC) substrates. J Electron Mater 40:2119–2125
86. Mei Y, Lu GO, Chen X et al (2011) Migration of sintered nano-silver die-attach material on alumina substrate between 250°C and 400°C in dry air. IEEE Trans Device Mater Reliab 11:316–322
87. Mei Y, Lu GO, Chen X et al (2011) Effect of oxygen partial pressure on silver migration of low-temperature sintered nano-silver die-attach material. IEEE Trans Device Mater Reliab 11:312–315

88. Herboth T, Gunther M, Fix A et al (2013) Failure mechanisms of sintered silver interconnections for power electronic applications. In: IEEE electronic components technology conference, pp 1621–1627
89. Kumpmann A, Guenther B, Kunze HD (1993) Thermal stability of ultrafine-grained metals and alloys. Mater Sci Eng A 168:165–169
90. Kobelev NP, Soifer YM, Andrievski RA et al (1993) Microhardness and elastic properties of nanocrystalline silver. Nanostruct Mater 2:537–544
91. Mei Y, Wang T, Cao X et al (2012) Transient thermal impedance measurements on low-temperature-sintered nanoscale silver joints. J Electron Mater 41:3152–3160
92. Ide E, Angata S, Hirose A et al (2005) Metal–metal bonding process using Ag metallo-organic nanoparticles. Acta Mater 53:2385–2393
93. Morita T, Ide E, Yasuda Y et al (2008) Study of bonding technology using silver nanoparticles. Jpn J Appl Phys 47:6615–6622
94. Yan J, Zou G, Wu AP et al (2012) Pressureless bonding process using Ag nanoparticle paste for flexible electronics packaging. Scr Mater 66:582–585
95. Lei TG, Calata JN, Lu GO et al (2010) Low-temperature sintering of nanoscale silver paste for attaching large-area ($>100\ mm^2$) chips. IEEE Trans Compon Packag Technol 33:98–104
96. Bai JG, Lu GQ (2006) A thermomechanical reliability study was conducted on a low-temperature sintered silver die attached SiC power device assemble. IEEE Trans Device Mater Reliab 6:436–441
97. Zou G, Yan J, Mu F et al (2011) Low temperature bonding of Cu metal through sintering of Ag nanoparticles for high temperature electronic application. Open Surf Sci J 3:70–75
98. Morisada Y, Nagaoka T, Fukusumi M et al (2010) A low-temperature bonding process using mixed Cu–Ag nanoparticles. J Electron Mater 39:1283–1288
99. Peng P, Hu A, Huang M et al (2012) Room-temperature pressureless bonding with silver nanowire paste: towards organic electronic and heat-sensitive functional devices packaging. J Mater Chem 22:12997–13001
100. Knoerr M, Schletz A (2010) Power electronics system integration for electric and hybrid vehicles. In: Proceedings of the 2010 6th International Conference integrated power electronics systems (CIPS), Nuremberg, 2010
101. Bai G, Lei G, Calata J, Lu GQ (2007) Control of nanosilver sintering attained through organic binder burnout. J Mater Res 22:3494–3500
102. Hu A, Guo JY, Alarifi H (2010) Low temperature sintering of Ag nanoparticles for flexible electronics packaging. Appl Phys Lett 97:1531171
103. Mayo MJ (1996) Processing of nanocrystalline ceramics from ultrafine powders. Int Mater Rev 41:85–115
104. Mayo MJ, Hague DC, Chen D (1993) Processing nanocrystalline ceramics for application in superplasticity. Mater Sci Eng A 166:145–159
105. Oestreicher A, Rohricha T, Wildenb J et al (2013) An innovative method for joining materials at low temperature using silver (nano)particles derived from [$AgO_2C(CH_2OCH_2)\ _3H$]. Appl Surf Sci 265:239–244
106. Kuramoto M, Ogawa S, Niwa M et al (2010) Die bonding for a nitride light-emitting diode by low-temperature sintering of micrometer size silver particles. IEEE Trans Compon Packag Manuf Technol 33:801–808
107. Ding L, Davidchack RL, Pan J (2009) A molecular dynamics study of sintering between nanoparticles. Comput Mater Sci 45:247–256
108. Jiu J, Zhang H, Koga S et al (2015) Simultaneous synthesis of nano and micro-Ag particles and their application as a die-attachment material. J Mater Sci Mater Electron 26:7183–7191
109. Kuramoto M, Kunimune T, Ogawa S et al (2012) Low-temperature and pressureless Ag-Ag direct bonding for light emitting diode die-attachment. IEEE Trans Compon Packag Manuf Technol 2:548–552

110. Kunimune T, Kuramoto M, Kunimune T et al (2012) High-conductivity adhesive for light-emitting diode die-attachment by low-temperature sintering of micrometer-size Ag particles. IEEE Trans Compon Packag Manuf Technol 2:909–915
111. Suganuma K, Sakamoto S, Kagami N et al (2012) Low-temperature low pressure die attach with hybrid silver paste. Microelecton Reliab 52:375–380
112. Schmitt W, Schafer M, Hagedorn HW (2010) Controlling the porosity of metal pastes for pressure free, low temperature sintering process. US2010/0051319A1, W.C. Heraeus, Hanau, 2010
113. Schmitt W, Dickel T, Stenger K (2009) Process and paste for contacting metal surfaces. US2009/0134206A1, W.C. Heraeus, Hanau, 2009
114. Morita T, Yasuda Y, Ide E (2008) Bonding technique using micro-scaled silver-oxide particles for in-situ formation of silver nanoparticles. Mater Trans 49:2875–2880
115. Knoerr M, Schletz A (2010) Power semiconductor joining through sintering of silver nanoparticles: evaluation of influence of parameters time, temperature and pressure on density, strength and reliability. In: International conference on integrated power electronics CIPS, Nurenberg, 2010
116. Ogura H, Maruyama M, Matsubayashi R et al (2010) Carboxylate-passivated silver nanoparticles and their application to sintered interconnection: a replacement for high temperature lead-rich solders. J Electron Mater 39:1233–1240
117. Sharma SK, Spitz J (1980) Hillock formation, hole growth and agglomeration in thin silver films. Thin Solid Films 65:339–350
118. Sakamoto S, Nagao S, Suganuma K (2013) Thermal fatigue of Ag flake sintering die-attachment for Si/SiC power devices. J Mater Sci Mater Electron 24:2593–2601
119. Heuck N, Langer A, Stranz A et al (2011) Analysis and modeling of thermomechanically improved silver-sintered die-attach layers modified by additives. IEEE Trans Compon Packag Manuf Technol 1:1846–1855
120. Lu J, Mu Y, Luo X (2012) A new method for soldering particle-reinforced aluminum metal matrix composites. Mater Sci Eng B Solid 177:1759–1763
121. Ozben T, Kilickap E, Cakır O (2008) Investigation of mechanical and machinability properties of SiC particle reinforced Al-MMCO. J Mater Process Technol 198:220–225
122. Zhang H, Nagao S, Suganuma K (2015) Addition of SiC particles to Ag die-attach paste to improve high-temperatures stability; grain growth kinetics of sintered porous Ag. J Electron Mater 44:3896–3903
123. Zhang H, Koga S, Jiu J et al (2015) Low temperature die attach based on sub-micron Ag particles and the high temperature reliability of sintered joints. In: Proceedings of the IEEE 65th electronic components and technology conference (ECTC), San Diego, 26–29 May 2015, pp 774–779
124. Zhang H, Nagao A, Suganuma K (2016) Thermostable Ag die-attach structure for high-temperature power devices. J Mater Sci Mater Electron 27:1337–1344
125. Yi L, Kyoung-Sik M, Haiying L, Wong CP (2004) Conductivity improvement of isotropic conductive adhesives with short-chain dicarboxylic acids. In: 54th proceedings on electronic components and technology conference, 2004, vol 2, pp 1959–1964
126. Chun-An L, Pang L, Hong-Ching L, Sea-Fue W (2007) Characterization of the low-curing-temperature silver paste with silver 2-ethylhexanoate addition. Jpn J Appl Phys 46:251–255
127. Kim I, Chun S (2011) Effects of solvent type on low-temperature sintering of silver oxide paste to form electrically conductive silver film. J Electron Mater 40:1977–1983
128. Jiu J, Zhang H, Nagao S et al (2016) Die-attaching silver paste based on a novel solvent for high-power semiconductor devices. J Mater Sci 51:3422–3430
129. Nishikawa H, Hirano T, Takemoto T, Terada N (2011) Effects of joining conditions on joint strength of Cu/Cu joint using Cu nanoparticle paste. Open Surf Sci J 3:60–64
130. Yan J, Zou G, Wu A et al (2012) Polymer-protected Cu-Ag mixed NPs for low-temperature bonding application. J Electron Mater 41:1886–1892

131. Magdassi S, Grouchko M, Kamyshny A (2010) Copper nanoparticles for printed electronics: routes towards achieving oxidation stability. Materials 3:4626–4638
132. Ding S, Jiu J, Tian Y et al (2015) Fast fabrication of copper nanowire transparent electrodes by a high intensity pulsed light sintering technique in air. Phys Chem Chem Phys 17:31110–31116
133. Mayousse C, Celle C, Carella A, Simonato JP (2014) Synthesis and purification of long copper nanowires. Application to high performance flexible transparent electrodes with and without PEDOT:PSS. Nano Res 7:315–324
134. Kobayashi Y, Shirochi T, Ysada Y et al (2012) Metal–metal bonding process using metallic copper nanoparticles prepared in aqueous solution. Int J Adhes Adhes 33:50–55
135. Joshi SS, Patil SF, Iyer V, Mahumuni S (1998) Radiation induced synthesis and characterization of copper nanoparticles. Nanostruct Mater 10:1135–1144
136. Ziegler KJ, Doty RC, Johnston KP, Korgel BA (2001) Synthesis of organic monolayer-stabilized copper nanocrystals in supercritical water. J Am Chem Soc 123:7797–7803
137. Morita T, Takesue M, Hayashi H et al (2016) Antioxidation properties and surface interactions of polyvinylpyrrolidone-capped zerovalent copper nanoparticles synthesized in supercritical water. ACS Appl Mater Interfaces 8:1627–1634
138. Yeh MS, Yang YS, Lee YP et al (1999) Formation and characteristics of Cu colloids from CuO powder by laser irradiation in 2-Propanol. J Phys Chem B 103:6851–6857
139. Liu Z, Bando Y (2003) A novel method for preparing copper nanorods and nanowires. Adv Mater 15:303–305
140. Wu S, Chen D (2004) Synthesis of high-concentration Cu nanoparticles in aqueous CTAB solutions. J Colloid Interface Sci 273:165–169
141. Lisiecki I, Billoudet F, Pileni MP (1996) Control of the shape and the size of copper metallic particles. J Phys Chem 100:4160–4166
142. Gao Y, Zhang H, Jiu J et al (2015) Fabrication of flexible copper pattern based on sub-micro copper paste by low temperature plasma technique. RSC Adv 5:90202–90208
143. Park B, Jeong S, Kim D et al (2007) Synthesis and size control of monodisperse copper nanoparticles by polyol method. J Colloid Interface Sci 311:417–424
144. Zhu J, Wang Y, Wang X, Yang X, Lu L (2008) A convenient method for preparing shape-controlled nanocrystalline Cu2O in a polyol or water/polyol system. Powder Technol 181:249–254
145. Lu C, Wey M, Fu Y (2008) The size, shape, and dispersion of active sites on AC-supported copper nanocatalysts with polyol process: the effect of precursor. Appl Catal A General 344:36–44
146. Cho C, Choi YW, Kang C, Lee GW (2007) Effects of the medium on synthesis of nanopowders by wire explosion process. Appl Phys Lett 91:141501–141503
147. Sarathi R, Sindhu TK, Chakravarthy SR (2007) Generation of nano aluminium powder through wire explosion process and its characterization. Mater Charact 58:148–155
148. Kirishnan S (2001) Preparation and low-temperature sintering of Cu nanoparticles for high-power devices. IEEE Trans Compon Packag Manuf Technol 2:587–592
149. Suryanarayana C (2001) Mechanical alloying and milling. Prog Mater Sci 46:1–184
150. Benavente E, Lozano H, Gonzalez G (2013) Fabrication of copper nanoparticles: advances in synthesis, morphology control, and chemical stability. Recent Pat Nanotechnol 7:108–132
151. Varshney R, Bhadaura S, Gaur MS (2012) A review: biological synthesis of silver and copper nanoparticles. Nano Biomed Eng 4:99–106
152. Ghorbani HR (2015) Biological and non-biological methods for fabrication of copper nanoparticles. Chem Eng Commun 202:1463–1467
153. Khodashenas B, Ghorbani HR (2014) Synthesis of copper nanoparticles: an overview of the various methods. Korean J Chem Eng 31:0105–1109
154. Draper GL, Dharmadasa R, Staata ME et al (2015) Fabrication of elemental copper by intense pulsed light processing of a copper nitrate hydroxide ink. ACS Appl Mater Interfaces 7:16478–16485

155. Kobayashi Y, Abe Y, Maeda T et al (2014) A metal-metal bonding process using metallic copper nanoparticles produced by reduction of copper oxide nanoparticles. J Mater Res Technol 3:114–121
156. Rathmell AR, Bergin SM, Hua Y et al (2010) The growth mechanism of copper nanowires and their properties in flexible, transparent conducting films. Adv Mater 22:3558–3563
157. Rathmell AR, Wiley BJ (2011) The synthesis and coating of long, thin copper nanowires to make flexible, transparent conducting films on plastic substrates. Adv Mater 23:4798–4803
158. Kevin M, Lim GYR, Ho GW (2015) Facile control of copper nanowire dimensions via the Maillard reaction: using food chemistry for fabricating large-scale transparent flexible conductors. Green Chem 17:1120–1126
159. Zhang D, Wang R, Wen M et al (2012) Synthesis of ultralong copper nanowires for high-performance transparent electrodes. J Am Chem Soc 134:14283–14286
160. Won Y, Kim A, Lee D et al (2014) Annealing-free fabrication of highly oxidation-resistive copper nanowire composite conductors for photovoltaics. NPG Asia Mater 6:e105
161. Yamakawa T, Takemoto T, Shimoda M et al (2013) Influence of joining conditions on bonding strength of joints: efficacy of low-temperature bonding using Cu nanoparticle paste. J Electronic Mater 42:1260–1267
162. Ishizaki T, Watanabe R (2012) A new one-pot method for the synthesis of Cu nanoparticles for low temperature bonding. J Mater Chem 22:25198–25206
163. Kim J, Rodriguez JA, Hanson JC et al (2003) Reduction of CuO and Cu_2O with H_2: H embedding and kinetic effects in the formation of suboxides. J Am Chem Soc 125:10684–10692
164. Lin Y, Hwang K (2010) Swelling of copper powders during sintering of heat pipes in hydrogen-containing atmospheres. Mater Trans 51:2251–2258
165. Champion Y, Bernard F, Guigue-Millot N, Perriat P (2003) Sintering of copper nanopowders under hydrogen: an in situ X-ray diffraction analysis. Mater Sci Eng A 360:258–263
166. Soininen PJ, Elers K, Saanila V et al (2005) Reduction of copper oxide film to elemental copper. J Electrochem Soc 152:G122–G125
167. Jang S, Seo Y, Choi J et al (2010) Sintering of inkjet printed copper nanoparticles for flexible electronics. Scr Mater 32:258–261
168. Yu E, Piao L, Kim S (2011) Sintering behavior of copper nanoparticles. Bull Kor Chem Soc 32:4099–4102
169. Wu C, Cheng S, Sheng Y, Tsao H (2015) Reduction-assisted sintering of micron-sized copper powders at low temperature by ethanol vapor. RSC Adv 5:53275–53279
170. Joo S, Hwang H, Kim H (2014) Highly conductive copper nano/microparticles ink via flash light sintering for printed electronics. Nanotechnology 25:265601
171. Dharmadasa R, Jha M, Amos DA, Druffel T (2013) Room temperature synthesis of a copper ink for the intense pulsed light sintering of conductive copper film. ACS Appl Mater Interfaces 5:13227–13234
172. Kim HS, Dhage SR, Shim DE, Hahn HT (2009) Intense pulsed light sintering of copper nanoink for printed electronics. Appl Phys A Mater Sci Process 97:791–798
173. Ryu J, Kim HS, Hahn HT (2010) Reactive sintering of copper nanoparticles using intense pulsed light for printed electronics. J Electron Mater 40:42–50
174. Luechinger NA, Athanassiou EK, Stark WJ (2008) Graphene-stabilized copper nanoparticles as an air-stable substitute for silver and gold in low-cost ink-jet printable electronics. Nanotechnology 19:445201
175. Kim C, Lee G, Rhee C, Lee M (2015) Expeditious low-temperature sintering of copper nanoparticles with thin defective carbon shells. Nanoscale 7:6627–6635
176. Yan JF, Zou GS, Hu A (2011) Preparation of PVP coated Cu NPs and the application for low-temperature Bonding. J Mater Chem 21:15981–15986
177. Lee C, Kim N, Koo J et al (2015) Cu-Ag core-shell nanoparticles with enhanced oxidation stability for printed electronics. Nanotechnolgy 26:455601

178. Cao W, Li W, Yin R, Zhou W (2014) Controlled fabrication of Cu-Sn core-shell nanoparticles via displacement reaction. Colloids Surf A: Physicochem Eng Asp 453:37–43
179. Jha M, Aharmadasa R, Draper GL et al (2015) Solution phase synthesis and intense pulsed light sintering and reduction of a copper oxide ink with an encapsulating nickel oxide barrier. Nanotechnology 26:175601
180. Kahler J, Heuck N, Wagner A (2012) Sintering of copper particles for die attach. IEEE Trans Compon Packag Manuf Technol 2:1587–1591
181. Peng Y, Yang C, Chen K et al (2012) Study on synthesis of ultrafine Cu–Ag core–shell powders with high electrical conductivity. Appl Surf Sci 263:38–44
182. Satoh T, Ishizaki T (2015) Enhanced pressure-free bonding using mixture of Cu and NiO nanoparticles. J Alloys Compd 629:118–123
183. Kim ST, Kuan YC (2014) Physical and electrical characteristics of silver-copper nanopaste as alternative die-attach. IEEE Trans Compon Package Manuf Technol 4:9–15
184. Watanabe R, Ishizaki T (2014) High-strength pressure-free bonding using Cu and Ni-Sn nanoparticles. Part Part Syst Charact 31:699–705
185. Fujimoto T, Ogura T, Sano T et al (2015) Joining of pure copper using Cu nanoparticles derived from CuO paste. Mater Trans 56:992–996
186. Park S, Uwataki R, Nagao S et al (2014) Low-pressure sintering bonding with Cu and CuO flake paste for power devices. In: 2014 I.E. 64th electronic components and technology conference (ECTC), pp 1179–1182
187. Grouchko M, Kamyshny A, Magdassi S (2009) Formation of air-stable copper-silver core-shell nanoparticles for inkjet printing. J Mater Chem 19:3057–3062
188. Park S, Sugahara T, Hatamura M et al (2015) Surface modification of Cu flakes through Ag precipitation for low-temperature pressureless sintering bonding. Mater Lett 151:68–71
189. Tsuji M, Hikino S, Tanabe R et al (2010) Syntheses of Ag/Cu alloy and Ag/Cu alloy core Cu shell nanoparticles using a polyol method. CrystEngComm 12:3900–3908
190. Kim N, Shi K, Jung I et al (2014) Ag-Cu bimetallic nanoparticles with enhanced resistance to oxidation: a combined experimental and theoretical study. J Phys Chem 118:26324–26331
191. Ishizaki T, Satoh T, Kuno A et al (2013) Thermal characterizations of Cu nanoparticle joints for power semiconductor devices. Microelectron Reliab 53:1543–1547
192. Sha CH, Lee CC (2012) Solid state bonding of silicon chips to silver buffer on copper substrates. IEEE Trans Compon Packag Manuf Technol 2:194–198
193. Smet V, Jamal M, Waldron F et al (2013) High-temperature die-attach technology for power devices based on thermocompression bonding of thin Ag films. IEEE Trans Compon Packag Manuf Technol 3:533–542
194. Kunimune T, Kuramoto M, Ogawa S et al (2013) Low-temperature pressure-less silver direct bonding. IEEE Trans Compon Packag Manuf Technol 3:363–369
195. Oh C, Nagao S, Suganuma K (2014) Pressureless bonding using sputtered Ag thin film. J Electron Mater 43:4406–4412
196. Oh C, Nagao S, Sugahara T, Suganuma K (2014) Hillock growth dynamics for Ag stress migration bonding. Mater Lett 137:170–173
197. Oh C, Nagao S, Suganuma K (2015) Silver stress migration bonding driven by thermomechanical stress with various substrates. J Mater Sci Mater Electron 26:2525–2530
198. Kim T, Howlader MMR, Itoh Y, Suga T (2003) Room temperature Cu-Cu direct bonding using surface activated bonding method. J Vac Sci Technol A 21:449–453
199. Tan CS, Lim DF, Singh SG et al (2009) Cu-Cu diffusion bonding enhancement at low temperature by surface passivation using self-assembled monolayer of alkane-thiol. Appl Phys Lett 95:192108
200. Tang Y, Chang Y, Chen K (2012) Wafer-level Cu-Cu bonding technology. Microelectron Reliab 52:312–320
201. Liu C, Lin H, Huang Y et al (2015) Low-temperature direct copper-to-copper bonding enabled by creep on (111) surfaces of nanotwinned Cu. Sci Rep 5:9734